Available online at www.sciencedirect.com
ScienceDirect
Journal of the European Ceramic Society 28 (2008) 2363–2388
www.elsevier.com/locate/jeurceramsoc

Phase equilibria in the refractory oxide systems of zirconia, hafnia and yttria with rare-earth oxides

E.R. Andrievskaya

Institute of Materials Science Problems, National Ukrainian Academy of Sciences, Krzhizhanovsky St. 3, Kiev 03142, Ukraine

Available online 5 March 2008

Abstract

The systematic study of phase equilibria in the ternary systems $HfO_2(ZrO_2)$–Y_2O_3–Ln_2O_3 has been first carried out. Phase reactions and crystallization of ceramic alloys in the binary systems ZrO_2–Ln_2O_3, HfO_2–Ln_2O_3, Y_2O_3–Ln_2O_3 and phase equilibria in the series of ternary systems HfO_2–Y_2O_3–Ln_2O_3 and ZrO_2–Y_2O_3–Ln_2O_3 have been developed at high temperature. The most general regularities of the phase reactions in liquid and solid states inherent in these systems have been considered dependent on lanthanide ion radii. Taking into account literature data and newly developed results in binary and ternary systems, the analysis of the main regularities revealed in the constitution of phase diagrams, particularly its dependence on lanthanide ionic radius, was carried out. It was shown that temperature and composition of eutectic reaction, temperature of the pyrochlore phase decomposition, lattice parameters of solid solutions and other parameters of the binary phases linearly depend on ionic radius of lanthanide. For the first time it has been found that the affiliation of lanthanide oxides to cerium or yttrium subgroups predetermines phase relations in the systems and topology of the ternary phase diagrams. The data obtained are the basis for the novel prospective ceramic materials for both structural and functional applications in energetic, medicine, nuclear industry, thermal barrier coatings, solid oxide fuel cells, etc.

Keywords: Zirconia; Hafnia; Yttria; Rare-earth oxides; Phase equilibria

1. Introduction

Stabilized zirconia is a unique material for many extensive applications: engineering ceramics, thermal barrier coatings, ceramic implants, electroceramics, high-temperature magneto-hydrodyhamic electrodes, fuel-cells, and oxygen sensors, etc. This variety is grounded on use of combination of mechanical, electrical, thermal and other properties.

The directionally solidified eutectic ceramic is one of the most attractive kinds of advanced zirconia-based ceramic materials demonstrating a unique combination of properties like high strength in combination with high fracture toughness. For oxide systems based on zirconia and alumina, the bending strength of 2.3 GPa remaining stable up to 1200 °C and fracture toughness of 4.3 MPa $m^{1/2}$ (at room temperature) were revealed if the eutectics were crystallized in the ceramic matrices.[1,2] Top level of the mechanical properties at room and high temperatures has been demonstrated in the carbide–boride-based systems. Paderno[3] has found that the directional solidified eutectic ZrB_2–LaB_6 ceramics allows obtaining the high toughness ceramic material with the fracture toughness of 20–25 MPa $m^{1/2}$ comparable with one for some steels and metallic alloys. This progress invoked new efforts in phase diagram research, under both equilibrium and non-equilibrium conditions. Certainly, the precise definition of the eutectic location is an important prerequisite for the directionally solidification work. It substantially depends on deviation from equilibrium.

This overview is dedicated to the study of the phase diagrams, phase equilibria in multicomponent ceramic compositions, especially those of them, which are close to the eutectic points. To make this work more systematic, the phase diagrams were studied in the series of the ternary systems $HfO_2(ZrO_2)$–Y_2O_3–Ln_2O_3, where symbol Ln means rare-earth metals. The overall purpose of the present research is the development of phase equilibria in the ternary systems based on ZrO_2, or HfO_2 and oxides of the IIIB subgroup (Y_2O_3 and rare-earth oxides (REO) such as La, Sm, Eu, Gd, Er) and properties of the phases existing in these systems. Double-doped zirconia or doped hafnia, the objects of ternary phase diagrams, which in turn were not studied well. Our efforts for the last decade to fill this space of knowledge resulted in the development of the

E-mail address: ragulya@ipms.kiev.ua.

0955-2219/$ – see front matter © 2008 Elsevier Ltd. All rights reserved.
doi:10.1016/j.jeurceramsoc.2008.01.009

ternary diagram. Thus, the present paper aims to show the main phase relations in the binary and ternary compositions considered prospective for new materials.[4–82]

From the practical use viewpoint, these systems are worth studying because of needs in new structural, functional ceramics and advanced coatings. In many applications, the ternary solid solutions of fluorite-type, C-type of the REO and intermediate pyrochlore-type phase are the targeted materials. In some cases, high strength of ceramics is necessary to combine with high ionic conductivity or low thermal conductivity. Such a combination is not attainable in a two-component solid solution, but becomes realistic in three-component systems. Summary of current and potential applications of ceramics based on the systems with different lanthanides $ZrO_2(HfO_2)$–Y_2O_3–Ln_2O_3 is presented in Table 1.

The phase relations in the ternary systems HfO_2–Y_2O_3–Ln_2O_3 and ZrO_2–Y_2O_3–Ln_2O_3 were studies in the wide range of temperature and concentrations using XRD, DTA in He at temperatures up to 2500 °C, thermal analysis in air (including solar furnace up to 3000 °C), petrography and electron microscopy.[83–87]

REO selected are representatives of lanthanides from the beginning, the middle and end of the raw. This allows deducing the main regularities of constitution in the series of the ternary diagrams $HfO_2(ZrO_2)$–Y_2O_3–Ln_2O_3. The comparison of the phase diagrams based on zirconia and hafnia permits elucidation the difference between the phase diagram constitution of the systems included the components—crystallographic analogs but differed by cation radius.

The crystallization of the alloys in the $ZrO_2(HfO_2)$–Y_2O_3–Ln_2O_3 systems was investigated using the data on liquidus and solidus surfaces. The crystallization paths for the alloys and the schematics of the reactions were constructed. The equilibrium phase diagrams have been deduced.

Basic interest to this research originates from the diversity of polymorphic modifications inherent to the mentioned oxides, intermediate phases and solid solutions stable or metastable, as well as from the effect of electronic structure and ionic radii of lanthanides on phase stability and boundaries of phase fields. The overview of general regularities in constitution of phase diagrams of the ternary systems $HfO_2(ZrO_2)$–Y_2O_3–Ln_2O_3 seems to be logically starting from the analysis of the bounded binary systems; then discuss several ternary systems and consider the character of phase crystallization, and then introduce some potential system for directional solidification study.

2. General characteristics and regularities of phase reactions in the systems HfO_2–Ln_2O_3 and ZrO_2–Ln_2O_3

Phase interaction of zirconia, hafnia and practically all lanthanide oxides (REO) (except Pm_2O_3, CeO_2) are thoroughly studied in the temperature range from 1500 °C up to melting 2900 °C.[4,57–60,63,65,67,68,88–221] At temperatures below 1500 °C these systems are studied a little, because the diffusion mobility is extremely low and the rate of solid solution and intermediate phase formation is infinitesimal. The phase diagrams of all the mentioned systems belong to the limited solubility type of diagrams. The main features inherent in these systems are polymorphism of REO, zirconia (hafnia) and intermediate phases as well as aleovalent character of ion substitution in the majority of solid solutions.[57,58,222–226] Ionic or electronic charge carriers compensate the excess charge on defects and this makes oxides sensitive with respect to environment (i.e. phase transformations become dependable on oxygen partial pressure).

The key feature of all solid solutions in these phase diagrams is the prevalence of a steric factor over energetic. The linear dependences of temperature–concentration coordinates versus ionic radii of rare-earth elements were revealed for many phase diagram elements. All phase diagrams of the binary systems $HfO_2(ZrO_2)$–Ln_2O_3 are of eutectic type (Figs. 1–4). The minimal liquidus temperature in the $ZrO_2(HfO_2)$–Ln_2O_3 systems correspond to the reactions of eutectic type $F + X \leftrightarrows L$ for lanthanide oxides of cerium subgroup and $F + H \leftrightarrows L$—for yttrium subgroup.

The coordinates (temperature and concentration) of eutectic points vary linearly with effective ionic radius of lanthanide. The temperature of reaction increases and the concentration of lanthanide oxide in eutectic point decreases with ion radius decrease (Table 2, Fig. 5).

Note, that under effective ionic radius in solid solution of substitution type $Me_{1-x}Ln_xO_2$ we understand the ratio of additivity: $R_{eff} = xR_{Ln}{}^{3+} + (1-x)R_{Me}{}^{4+}$, where ч is a concentration in mol%, R is the cation radius. The linear approximation is sufficient, taking into account low accuracy of temperature measurement above 2000 °C, as well as the tendency for some oxides to change oxidation degree in vacuum or inert gas medium. The eutectic reactions in the systems with HfO_2 occur at temperatures 50–100 °C higher, than that in systems based on ZrO_2, which correspond to difference in melting points for pure hafnia and zirconia (Table 2).

In the selected systems, the substitution-type solid solutions are known to be formed by components and intermediate phases. The substantial phenomenon in the solid solutions is the non-stoichiometry. Thus, the solid solutions based on cubic modifications of $HfO_2(ZrO_2)$ form so called "defect fluorite" structure.[227] The substitution of hafnium or zirconium ions by lanthanide ion leads to increased concentration of oxygen vacancies—the defects compensating the lack of positive ionic charge in the cation sublattice.[228] The formation of solid solutions also occurs by substitution of lanthanide ion by hafnium or zirconium ion, provided the electron compensation of excess charge.[62]

The model of substitution-type solid solution based on MeO_2 (Me = Hf, Zr) can be presented by Kröger-Vink formula: $Me^{4+}{}_{1-x}Ln^{3+}{}_xO^{2-}{}_{2-(x/2)}$. This formula seems to be correct for all three types of solid solutions based on monoclinic (M), tetragonal (T) and cubic (fluorite-type, F)—polymorphs of MeO_2. Additives of the REO markedly decrease temperatures of phase transformations $T \leftrightarrows M$ and $T \leftrightarrows F$ in hafnia and zirconia. In the series of phase diagrams, temperature of melting and solid-state transformations directly depends on the ratio between ionic radii of cations $r_{Hf}{}^{4+}/r_{Ln}{}^{3+}$. The solubility in the monoclinic phase, as a rule, does not exceed 2 mol%, and in the tetragonal it is less

Table 1
High performance applications based on zirconia[87]

Function	Materials	Applications
Electrical insulation	ZrO_2, Al_2O_3	IC circuit substrate
Ion-conductivity	β-Al_2O_3, Y_2O_3–ZrO_2, CeO_2, Gd_2O_3–CeO_2	Solid electrolytes (sodium battery), oxygen sensor, fuel cell membrane, gas generator, membrane reactor
Chemical ceramics	ZrO_2, TiO_2, CeO_2, rare-earth oxides	Chemical sensor, catalyst, catalyst support, desiccant, gas, adsorption/storage
Structural ceramics	ZrO_2(TZP), cordierite, Al_2TiO_5,	Automotive, heat exchangers, metal filters, thermal barrier coatings, diesel port liners
Biological ceramics	Doped zirconia	Artificial valves for hearts
Thermal insulation	$Ln_2Zr_2O_7$, $CaAl_2O_4$	Refractory, TBC
Neutrons absorption	$HfO_2(ZrO_2)$–$Y_2O_3(Eu_2O_3)$	Rods for nuclear reactors

than 5 mol% Ln_2O_3. The fluorite-type solid solutions dissolve up to 80 mol% REO. The excess concentration of compensating vacancies in the oxygen sublattice and presence of ions larger than zirconium or hafnium ions, both promote transformation of martensitic type in ZrO_2 and HfO_2 at temperatures lower than 1170 and 1830 °C in pure oxides, respectively. The effect of size and charge of added ion on properties of solid solutions based on monoclinic modifications of REO and ZrO_2 were studied by Yoshimura et al. [179,229–231] In the case of lanthanide oxides, the lattice parameters of monoclinic ZrO_2 solid solutions dissolving 2 mol%, Ln_2O_3, varies linearly with ionic radius of lanthanide (Fig. 6). The periods *a*, *b*, *c* and volume of elementary cell increase isotropically, and the angle of monoclinity decreases with ion radius increase.

The solid solution based on tetragonal zirconia (T-ZrO_2), suffers transformation T ⇆ M at temperature on 400 °C lower than in pure MeO_2. Nonequivalence of sites in low-symmetrical lattices (such as monoclinic and tetragonal) result in substantial deformations of lattices and phase transformations stimulated by doping. In the homogeneity field of T-ZrO_2, the period of elementary cell linearly depends on lanthanide ionic radius (Fig. 7).[179]

The fluorite-type solid solution with cubic lattice is the most stable in these systems and demonstrates maximal solubility among them. The solubility limit of REO in F-HfO_2 (ZrO_2) depends on lanthanide ionic radius (Table 3). In the systems ZrO_2–Ln_2O_3, the lattice parameter *d* of the fluorite-type solid solutions of the same concentration changes linearly with ionic radius of lanthanide and can be approximated by empirical equation: [228,231]

$$d = 5.120 + [0.212(R_{Ln}{}^{3+} - R_{Zr}{}^{4+}) - 0.0023]m$$

where *m* is the mol% of REO, $R_{Ln}{}^{3+}$ and $R_{zr}{}^{4+}$ are the radii of corresponding ions. The calculated approximation fits the experimental values of *d*.

Features of transformation from cubic to tetragonal phases were investigated theoretically and experimentally by Katamura et al.[214,215] The kinetics and mechanisms which control the formation of fluorite solid solutions in the binary and ternary systems were studied by Glushkova and Duran.[66,232–234] They showed the competition between diffusion controlled mass transport and nucleation of new phase when fluorite-type solid solution transformed into the ordered pyrochlore-type phases.

The solid solutions based on polymorphs of REO are also of substitution type, where the electron-ionic compensation of excessive charge takes place.[62,235] In case of interstitial oxygen ion, the compensation of positive charge occurs and corresponding to the formula: $Ln^{3+}{}_{2-x}Me^{4+}{}_xO^{2-}{}_{3+0.5x}$.

The solubility of hafnia or zirconia in hexagonal (A) and monoclinic (B) modifications of REO is small. The widest homogeneity field belongs to the solid solutions based on C-type of REO. These solid solutions have cubic structure, the derivative from the fluorite-type structure. For the lanthanides of cerium subgroup, however, this phase was not revealed in high-temperature fields of the phase diagrams, but low-temperature fields were not studied yet because of extremely slow diffusion activity and abnormally long duration of homogenization.

2.1. Intermediate phases in the systems $HfO_2(ZrO_2)$–$Ln_2O_3(Y_2O_3)$

The analysis of existing data has revealed a considerable similarity between binary systems based on hafnia and zirconia. In the systems $HfO_2(ZrO_2)$–$Ln_2O_3(Y_2O_3)$, formation of several intermediate phases were found: phases with crystalline structure of the pyrochlore-type (*Fd*3*m*, stoichiometry formula $Ln_2Hf_2O_7(Ln_2Zr_2O_7)$; a phase with hexagonal structure (R3, formulated as $Ln_4M_3O_{12}$), as well as the phases of perovskite-type cubic structure with rhombic distortions (sD^{16}_{2h} −*Pbnm*, formulated as $LnMeO_3$).

2.2. The pyrochlore-type phases

It is well known that the ionic conductivity of solid solutions of fluorite-type passes through the maximum value, which corresponds to the maximum concentration of the mobile defects—anion vacancies, for instance. At high concentration of dopant, the vacancies are turned for integration into sluggish clusters such as bi-, tri-vacancies, etc. The defect structure enables to initiate rearrangement of the lattice as a whole, ordering, and formation of new phase, as it was found in case of ordering the pyrochlore-type solid solutions. This ordering

Table 2
The coordinates of invariant points in the systems HfO_2–Ln_2O_3 and ZrO_2–Ln_2O_3

Ln_2O_3	Systems HfO_2–Ln_2O_3						Systems ZrO_2–Ln_2O_3 [58]		
	Ionic radius, by Ahrrenius (nm)	R_{ef} (nm)	Composition eutectic HfO_2 (mol%)	Temperature of eutectic (°C)	Composition of peritectic HfO_2 (mol%)	Temperature of peritectic (°C)	R_{ef} (nm)	Composition eutectic	Temperature of eutectic (°C)
La	0.114	0.1014	35	2070	–	–	0.10068	0.37	1980
			77	2330 [103]					
Ce	0.107	0.0983	30	–	–	–	–	–	–
Pr	0.106	0.09816	28	2125	45	∼2200	0.09704	0.32	2100
			75	2420 [103]					
Nd	0.104	0.09698	27	2140 [103]	65	2450	0.0962	0.30	2120
					∼48	∼2270			
Sm	0.102	0.09428	26	2240 [122]	67	2550	0.0945	0.25	2180
					∼52	∼2335			
Eu	0.098	0.093	25	2150 [139]			0.0928	0.26	2130 [196]
Gd	0.097	0.09282	22	2310 [122]	–	–	0.09244	0.24	2260
Tb	0.093	0.09015	19	2300 [122]	∼30	∼2350	0.08955	0.23	2250
Dy	0.092	0.08934	19	2310 [122]	∼32	∼2390	0.08892	0.22	2280
Ho	0.091	0.08905	15	2340 [154]	∼31	∼2380	0.08866	0.18	2300
Y	0.092	0.08976	16	2400 [154]	∼30	2430	0.08976	0.16	2360
Er	0.089	0.08735	15	2360 [154]	∼30	∼2400	0.08702	0.18	2350
Tm	0.087	0.08574	14	2380 [154]	∼33	∼2460	–	–	–
Yb	0.086	0.08496	13	2430 [154]	∼35	∼2500	0.0848	0.15	2410
Lu	0.085	0.08416	–	–	12	2510 [154]	–	–	–

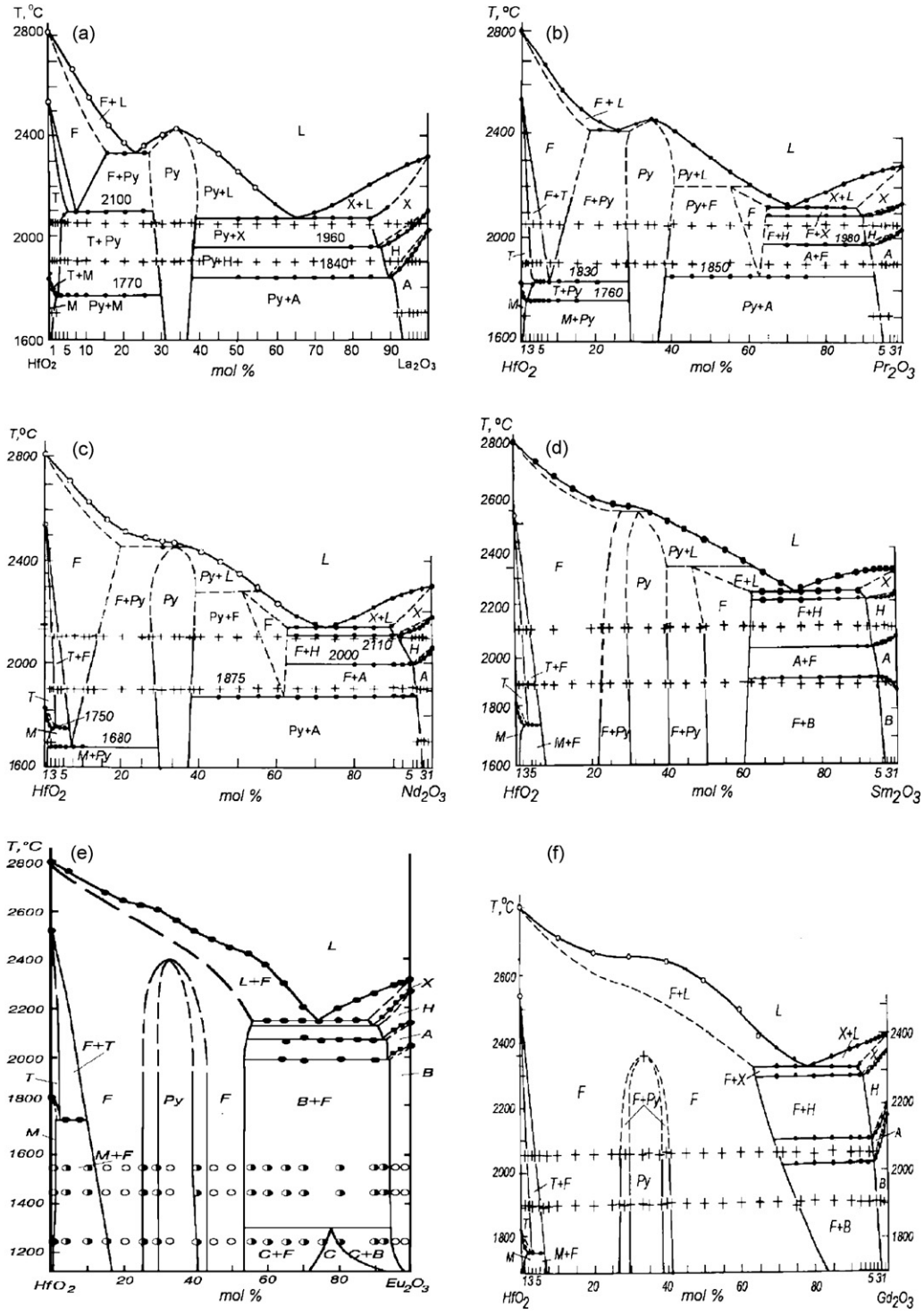

Fig. 1. Phase diagrams of the binary systems with hafnia and lanthanide oxides from lanthana to gadolinia: (a) HfO_2–La_2O_3,[103] (b) HfO_2–Pr_2O_3,[103] (c) HfO_2–Nd_2O_3,[103] (d) HfO_2–Sm_2O_3,[122] (e) HfO_2–Eu_2O_3, (f) HfO_2–Gd_2O_3;[122] (◯) DTA in helium; (+) annealing and quenching technique, (●) thermal analysis in air under solar furnace; (◯) single-phase regions, (◑) two-phase regions by the data of XRD and annealing and quenching.

occurs by the way of cation rearrangement, distributed in the disordered solid solution of the fluorite-type and filling cites in the pyrochlore lattice, as well as by the oxygen ion shifting in the anion sublattice, i.e. by changing of the oxygen ion's coordination and abrupt decreasing of oxygen vacancies concentration.[236] All these pyrochlore-type phases possess wide homogeneity fields, but much narrower ones than fluorite-type solid solutions. The deviation from stoichiometry in the $Ln_2Hf_2O_7$ phase appears, when x ions of Hf^{4+} are substituted by x ions of Ln^{3+}. On substitution, the $x/2$ additional oxygen vacancies are formed $Ln_{2+x}Hf_{2-x}O_{7-(x/2)}$. When the Ч′ ions of Ln^{3+} are substituted by Ч′ ions of Hf^{4+} the number of oxygen vacan-

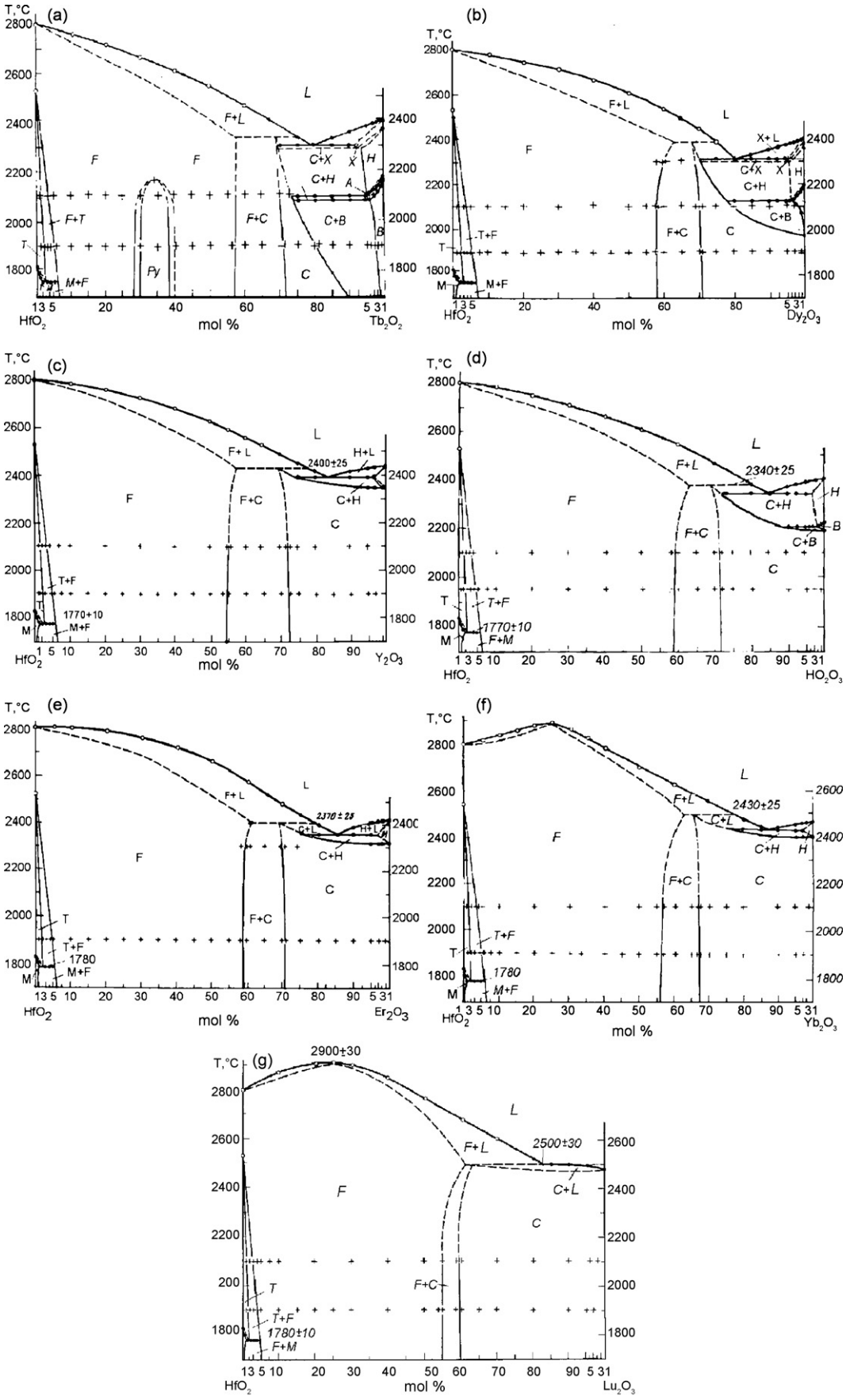

Fig. 2. Phase diagrams of the binary systems with hafnia and lanthanide oxides from terbia to lutetia: (a) HfO_2–Tb_2O_3,[122] (b) HfO_2–Dy_2O_3,[122] (c) HfO_2–Y_2O_3,[154] (d) HfO_2–Ho_2O_3,[154] (e) HfO_2–Er_2O_3,[154] (f) HfO_2–Yb_2O_3,[154] (g) HfO_2–Lu_2O_3.[154]

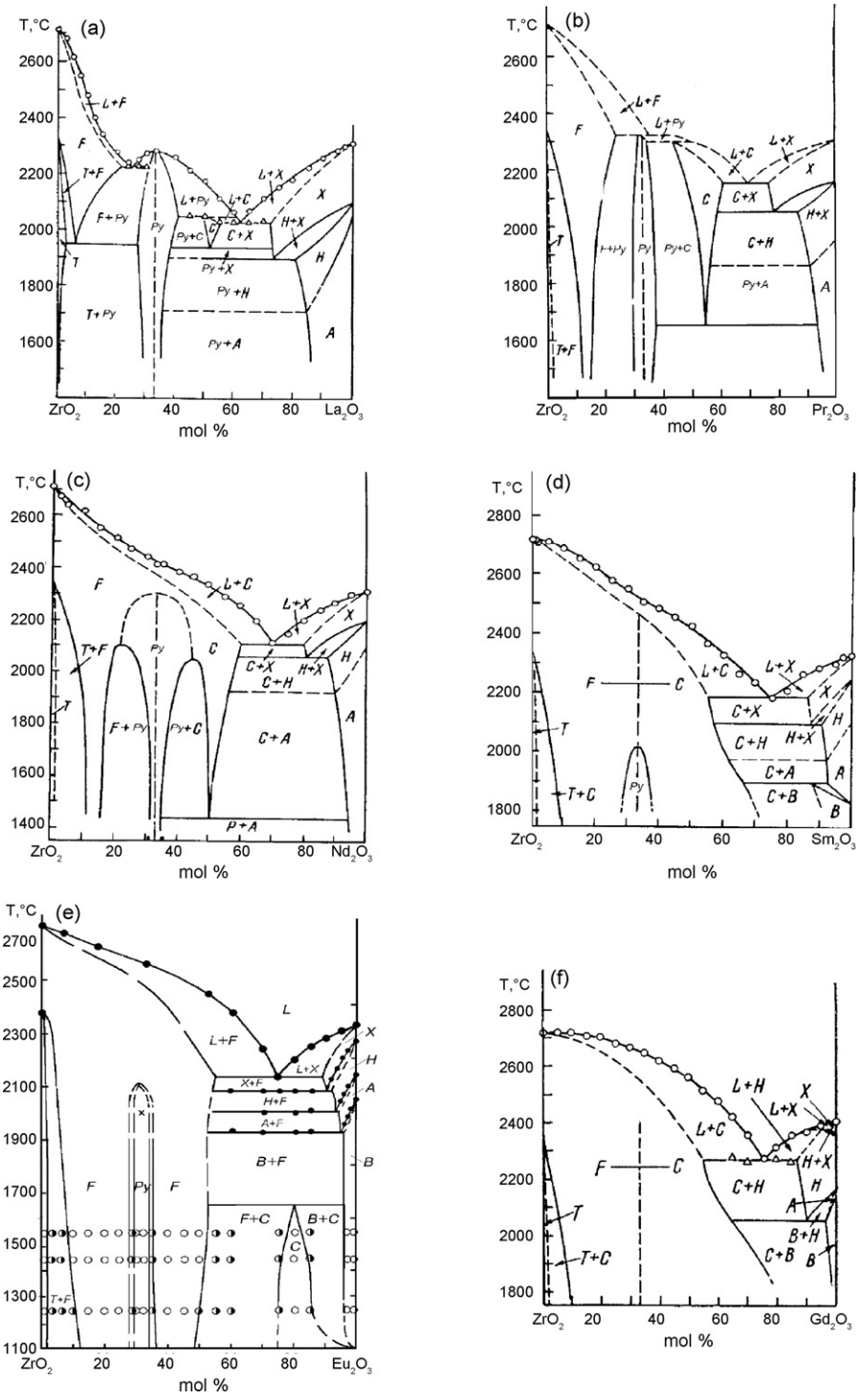

Fig. 3. Phase diagrams of the binary systems with hafnia and lanthanide oxides from lanthana to gadolinia: (a) ZrO_2–La_2O_3,[63] (b) ZrO_2–Pr_2O_3,[63] (c) ZrO_2–Nd_2O_3,[63] (d) ZrO_2–Sm_2O_3,[63] (e) ZrO_2–Eu_2O_3, (f) ZrO_2–Gd_2O_3;[63] (◯) experimental points; (●) thermal analysis in air under solar furnace; (◯) single-phase regions, (◑) two-phase regions by the data of XRD and annealing and quenching.

cies in the anion sublattice of $Ln_{2-x}Hf_{2+x}O_{7-(x/2)}$ decreases in Ч′/2.[235] The pyrochlore-type phases demonstrate concentration limits of stability, which are shown in Tables 4 and 5, Fig. 8. The pyrochlore-type phases and their solid solutions are formed by zirconia or hafnia with cerium subgroup of REO (from La to Gd), while the REO of yttrium subgroup form disordered solid solutions of fluorite type.[237] The thermodynamic stability of the pyrochlore type compounds can be determined using empirical rule, which identifies the ratio between ionic radii $R = (r^{3+}_{Ln}/r^{4+}_{Hf})$, which must be higher than 1.2. In accordance with Colong,[235] the average ionic radii for the pyrochlore-type phases can be approximately calculated by additive rule:

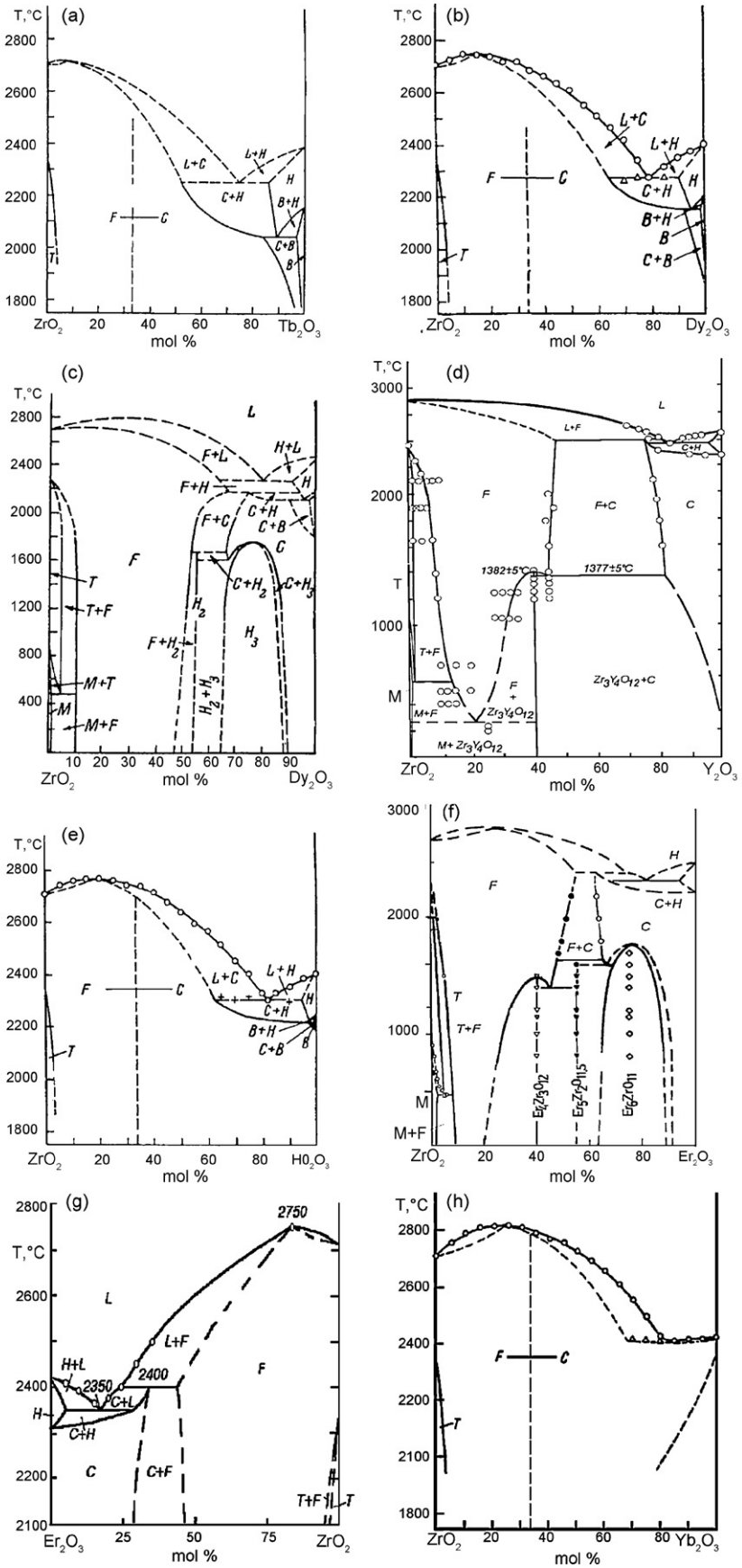

Fig. 4. Phase diagrams of the binary systems with hafnia and lanthanide oxides from terbia to lutetia: (a) ZrO_2–Tb_2O_3,[63] (b and c) ZrO_2–Dy_2O_3,[63,194] (d) ZrO_2–Y_2O_3,[156] (e) ZrO_2–Ho_2O_3,[63] (f and g) ZrO_2–Er_2O_3,[219,221] (h) ZrO_2–Yb_2O_3.[63]

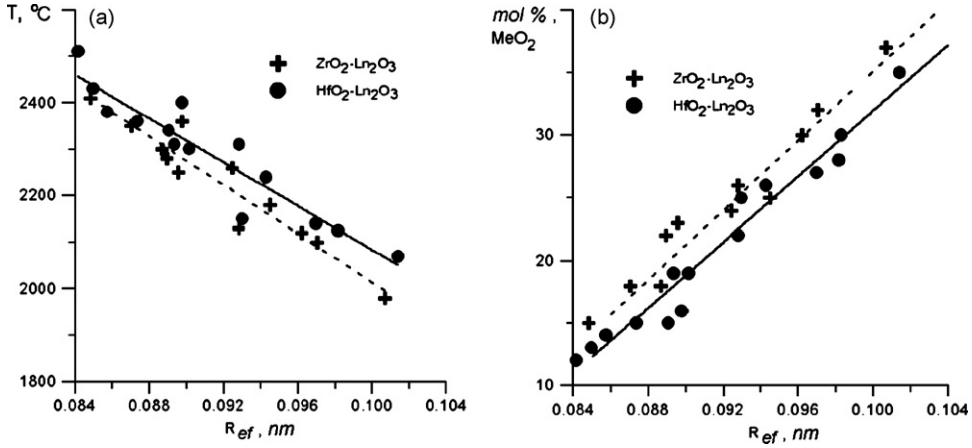

Fig. 5. Dependence of melting temperature (a) and composition (b) for eutectics in the systems MeO_2–Ln_2O_3 vs. effective ionic radius of lanthanide (Table 2, R_{Ln}^{3+} and R_{Me}^{4+} are taken by Ahrens scale [257]).

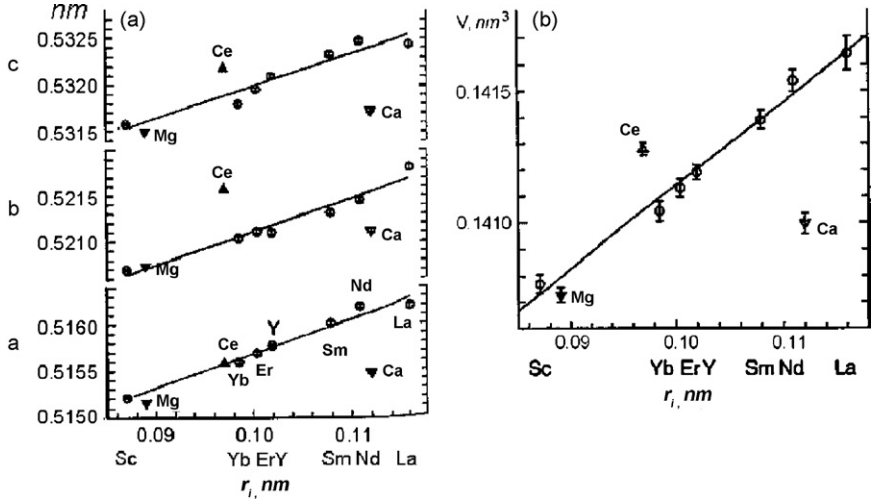

Fig. 6. Dependence of lattice parameters (a) and volume of elementary cell (b) for the solid solution based on monoclinic ZrO_2 vs. ionic radius of dopant.[230]

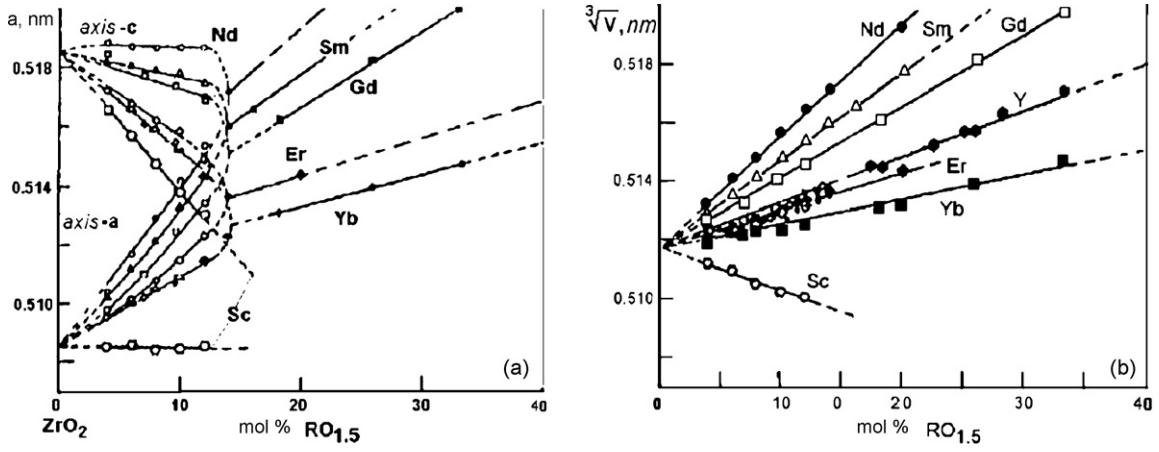

Fig. 7. Dependence of lattice parameters (a) and volume of elementary cell (b) for the solid solution based on tetragonal ZrO_2 versus ionic radius of dopant.[179]

Table 3
The solubility of components in the systems HfO_2–Ln_2O_3

Ln^{3+}	Ionic radius, by Ahrens (nm)	Limit of solubility (mol%)									Source
		Py	M	T	F	X	H	A	B	C	
La	0.114	27–40	2	5	15	15	12	10	–	–	103
Pr	0.107	27–40	2	4	17/65	12	10	8	–	–	103
Nd	0.104	27–39	2	3	18/63	11	9	5	–	–	103
Sm	0.100	29–39	2	3	27/62	10	8	6	4	–	122
Eu	0.099	30–38	1.5	3	55	10	8	5	4	–	139
Gd	0.095	30–38	1.5	2.5	83/64	10	9	5	3.5	–	122
Tb	0.093	30–38	1.5	2.5	58	8	5	4	3	30	122
Dy	0.092	–	1.5	2.5	62	5	4.5	–	3	32	122
Ho	0.091	–	1	2.0	63	–	4	–	2	30	154
Y	0.092	–	1	2.0	57	–	3	–	–	30	154
Er	0.089	–	1	2.0	60	–	3	–	–	30	154
Yb	0.086	–	1	2.0	62	–	2.5	–	–	35	154
Lu	0.085	–	1	2.0	60	–		–	–	40	154

Table 4
Properties of the $Ln_2Hf_2O_7$ phases[58]

Phase	a (nm)	$-\Delta H^\circ_f$ (kJ/mol)	T_m (K)	D_{mes} (g/cm^3)	TEC $\times 10^{-6}$/°
$La_2Hf_2O_7$	1.0776	–	2560	7.84	7.85
$Pr_2Hf_2O_7$	1.0960	104	2610	7.90	9.13
$Nd_2Hf_2O_7$	1.0648	85	2730	8.11	9.27
$Sm_2Hf_2O_7$	1.0568	82	2760	8.20	10.60
$Eu_2Hf_2O_7$	1.0540	–	2735	8.29	10.82
$Gd_2Hf_2O_7$	1.0502	41	2790	8.34	–

Table 5
Properties of the phases $Ln_2Zr_2O_7$[58]

Phase	a (nm)	$-\Delta H^\circ_f$ (kJ/mol)	T_m (K)	D_{mes} (g/cm^3)	TEC $\times 10^{-6}$/°
$La_2Zr_2O_7$	1.0808	126.1	2160	5.89	9.129
$Pr_2Zr_2O_7$	1.0714	120.3	2220	6.14	5.65
$Nd_2Zr_2O_7$	1.0668	111.0	2320	6.28	11.717
$Sm_2Zr_2O_7$	1.0594	106.8	2350	6.48	10.733
$Eu_2Zr_2O_7$	1.0554	80.0	2350	6.63	9.347
$Gd_2Zr_2O_7$	1.0528	75.8	2450	6.69	11.519

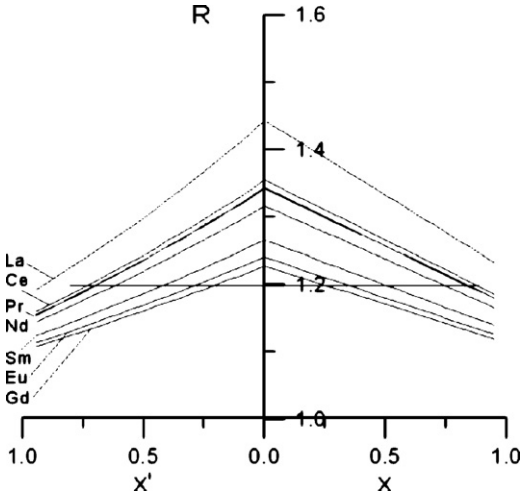

Fig. 8. Calculated scheme for determination of the homogeneity field size for the phases of pyrochlore type in the systems HfO_2–Ln_2O_3.[235]

$$r_{Me} = r_{Hf_{2-x}Ln_x} = \frac{1}{2}[(2-x)r_{Hf} + xr_{Ln}]$$

$$r'_{Me} = r_{Ln_{2-x'}Hf_{x'}} = \frac{1}{2}[(2-x')r_{Ln} + x'r_{Hf}]$$

$$R_l = \frac{r_{Ln}}{r_{Me}} = \frac{2r_{Ln}}{(2-x_l)r_{Hf} + x_l r_{Ln}} = 1.2$$

$$R = \frac{r^{3+}_{Ln}}{r^{4+}_{Hf}} \geq 1.2 \text{ (for the pure pyrochlore phases)}$$

$$R_l = \frac{r'_{Me}}{r_{Hf}} = \frac{(2-x'_l)r_{Ln} + x'_l r_{Hf}}{2r_{Hf}} = 1.2$$

where R_l is the ratio of average radii for ions taking into account their substitution. The boundary value $R_l = 1.2$ responds to two values of x_l and x'_l. The results of calculation are presented in Fig. 8. The boundary ratio is correct for gadolinium hafnate but wrong for terbium hafnate.

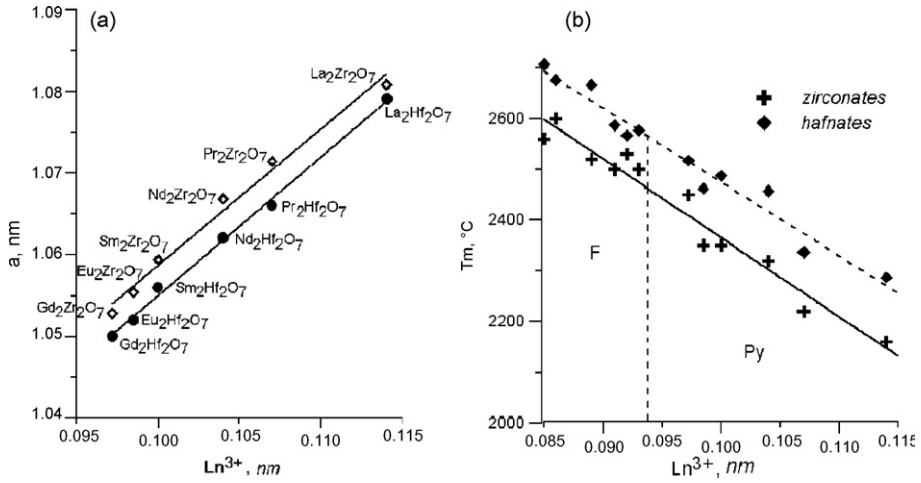

Fig. 9. The lattice parameter of the ordered phases $Ln_2Hf_2O_7$ (●) $Ln_2Zr_2O_7$ (◊) (a) and melting temperatures corresponding to the compositions 33.3 mol% Ln_2O_3 66.7 mol% ZrO_2 (b) vs. ionic radius of lanthanide.

The ordered phase $La_2Zr_2O_7$ is stable up to its melting temperature, the $Nd_2Zr_2O_7$ exists at approximately 2300 °C and lower, while the $Gd_2Zr_2O_7$ is stable at temperatures less than 1500 °C.[238] In this series of pyrochlore-type hafnates and zirconates we found a linear increasing of their lattice parameters, and linear decreasing of their melting temperatures with increasing of ionic radius of Ln^{3+} as shown in Fig. 9.

The most thermodynamically stable phase is the lanthanum zirconate (hafnate), having minimal melting temperature in the series $Ln_2Zr_2O_7$($Ln_2Hf_2O_7$) and the loosest lattice (the largest lattice parameter). Lanthanides from the end of the series do not form ordered compounds with pyrochlore-type lattice, because the spatial factor is not appropriate to order ions in the lattice. Recently the phenomenon of ordering/disordering was studied in the pyrochlore phases by molecular static methods.[239,240] It was shown, that the enthalpy of ordering quickly decreases with ion radii increase in site B (B corresponds to Zr^{4+} and Hf^{4+}) and decrease of Frenkel's pair formation energy (oxygen vacancy in the site 48f + interstitial ion in position 8a of the pyrochlore lattice). This is clear, that the ionic and electronic conductivity can be increased.[241,242] This rule will be working in the ternary systems, if high-enthalpy phases of pyrochlore would be doped with disordering additives.

3. General characteristics and phase reactions in the systems Ln_2O_3–Y_2O_3

Existing data [66,243–256] and results of the present research allow several conclusions concerning regularities in phase diagrams of the systems REO–yttria. In these systems, the solid solutions based on polymorphous modification of REO were found (Fig. 10). The fields of mutual solubility of components in these systems are defined by steric factor, which in turn, is defined by the size of cations and structure of REO. The coordinates of invariant points in the phase diagrams of the systems Ln_2O_3–Y_2O_3 are presented in Table 6 and Fig. 10.

The additives of Y_2O_3 to light lanthanides (La_2O_3, Pr_2O_3, Nd_2O_3) promote formation of the solid solutions based on B-form of REO, which has not been found in pure oxides.[223,225] In the systems with REO from the middle of the series (Sm_2O_3, Eu_2O_3, Gd_2O_3, Dy_2O_3), the widening of homogeneity fields was revealed for C-type of solid solutions. In the systems with heavy REO, the solid solutions of C-type demonstrate unlimited solubility in the wide range of temperature.[246,247]

High-temperature phase H is known in several REO and yttria. In all studied systems, the continuous solubility in the H-Ln_2O_3 has been observed. Polymorphous modification X, contrary to form H, was found for lanthanides of cerium subgroup, and extension of the homogeneity fields for the X-phase decreases from La_2O_3 to Gd_2O_3. Solid solutions based on X- and H-forms of REO cannot be quenched from high temperatures.

Equimolar compositions of REO[59] are able to be ordered and intermediate phases of perovskite type remains stable if cation radii difference is greater than or equal to 0.022 nm. Amid several systems Ln_2O_3–Y_2O_3, this condition is satisfied for the diagram La_2O_3–Y_2O_3, where this phase was definitely found ($LaYO_3$). However, as this ratio is equal to the boundary value, the $LaYO_3$ is stable in solid state. In the other systems, the $LnYO_3$ were not found. In the ternary systems, the substitution of large size cation Ln^{3+} by Zr^{4+} of smaller size can be a reason for stabilization of $LnYO_3$.

3.1. Stability intermediate phases and prognosis phase equilibria in the systems Ln_2O_3–Y_2O_3

Following the regularities of constitution, one can forecast the constitution of unknown six diagrams. Such a prognosis is important for defining the surface topology of the liquidus surface, because the elements of ternary diagrams situated close to the bounded binary systems Ln_2O_3–Y_2O_3, strongly contribute to the topology of the liquidus surface, existence and position of invariant points. Temperature of invariant points and extreme points on liquidus curves, points on solidus, X ⇆ H transition and solid-state reactions in the binary systems Ln_2O_3–Y_2O_3 change linearly with lanthanides ionic radius (Figs. 11 and 12). These dependences work the best for oxides of cerium sub-

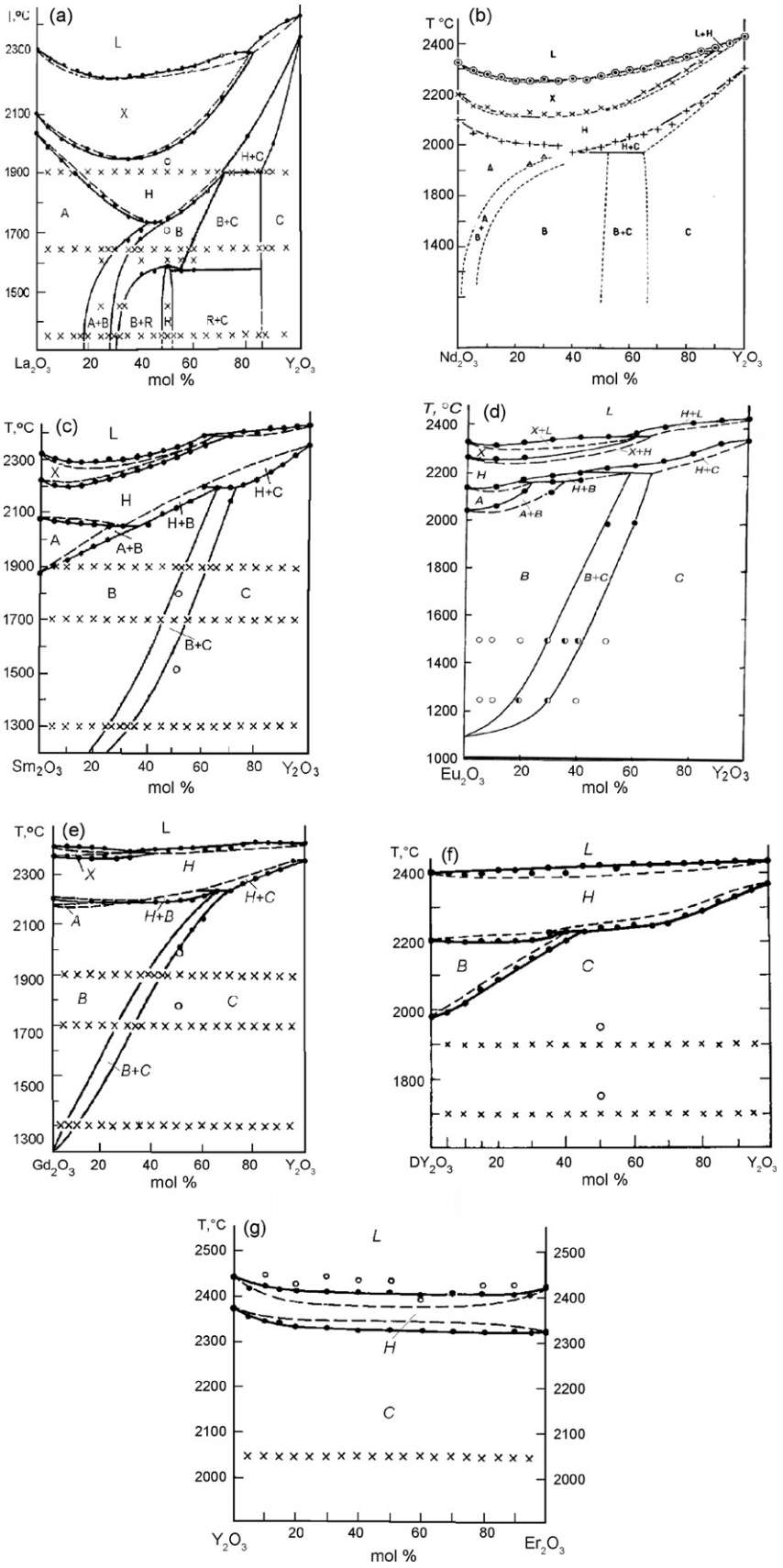

Fig. 10. Phase diagrams of the binary systems with yttria and lanthanide oxides: (a) La_2O_3–Y_2O_3,[244] (b) Nd_2O_3–Y_2O_3,[255] (c) Sm_2O_3–Y_2O_3,[245] (d) Eu_2O_3–Y_2O_3, (e) Gd_2O_3–Y_2O_3,[245] (f) Dy_2O_3–Y_2O_3,[246] (g) Er_2O_3–Y_2O_3[247]; (●) DTA in helium and thermal analysis in air under solar furnace; (◯) high-temperature XRD; (×) annealing and quenching technique; (◯) single-phase regions, (◑) two-phase regions by the data of XRD and annealing and quenching.

Table 6
The coordinates of invariant points for the systems Ln_2O_3–Y_2O_3

Systems	Ionic radius Ln^{3+}, by Ahrens (nm)	Coordinates of peritectisc L + H ⇄ X, p (eutectics, e)		Coordinates of minimum on liquidus		Coordinates of minimum X ⇄ H		Coordinates of peritectoid H + C ⇄ B		Coordinates of eutectoid, H ⇄ A + B, e (peritectoid, *p*)	
		Y_2O_3 (mol%)	*T* (°C)	Y_2O_3 (mol%)	*T* (°C)	Y_2O_3 (mol%)	*T* (°C)	Y_2O_3 (mol%)	*T* (°C)	Y_2O_3 (mol%)	*T* (°C)
La_2O_3–Y_2O_3	0.114	83	2310 (p) [244]	30	2215	35	1950	71	1900	45	1730
Pr_2O_3–Y_2O_3*	0.106	70	2354 (p)	21	2214	22	2093	67	2062	35	1934
Nd_2O_3–Y_2O_3	0.104	84	2370 (p)	30	2250	25	2120	51	1960	N/A	N/A
Sm_2O_3–Y_2O_3	0.100	60	2400 (p) [245]	15	2290	10	2200	65	2200	30	2050
Eu_2O_3–Y_2O_3	0.098	58	2370 (p) [248]	10	2310	10	2250	58	2210	23	2160 (p)
Gd_2O_3–Y_2O_3	0.097	30	2390 (p) [245]	10*	2324*	5*	2254	65	2230	25	2180
Tb_2O_3–Y_2O_3*	0.093	6*	2420 (p)	–	–	–	–	–	–	–	–
Dy_2O_3–Y_2O_3	0.092	–	–	–	–	–	–	40	2230 [246]	–	
Ho_2O_3–Y_2O_3*	0.091	–	–	–	–	–	–	10	2240	–	–
Er_2O_3–Y_2O_3	0.089	–	–	–	–	–	–	–	–	–	–
Tm_2O_3–Y_2O_3	0.087	–	–	–	–	–	–	–	–	–	–
Yb_2O_3–Y_2O_3	0.086	–	–	–	–	–	–	–	–		–
Lu_2O_3–Y_2O_3	0.085	–	–	–	–	–	–	–	–	–	–

Note: (*) calculated data.

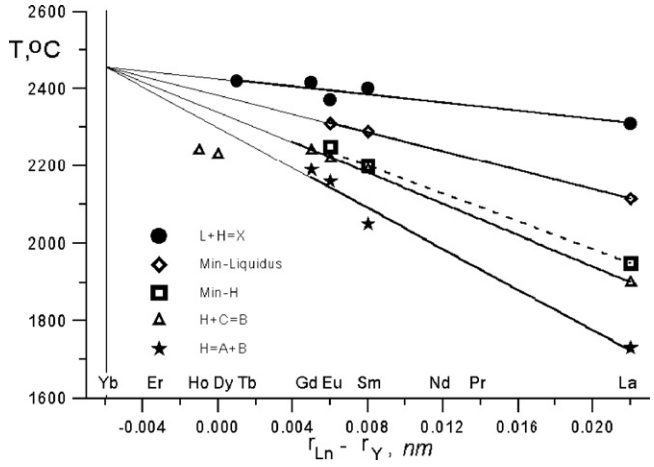

Fig. 11. Characteristic temperatures of invariant points in the binary systems Ln_2O_3–Y_2O_3 as a function of lanthanide ionic radius.

groups, while for REO of yttrium subgroup one can observe the deviations. These discrepancies originate from the various polymorphs of oxides for cerium and yttrium subgroup. Note the strait lines approximating the experimental points cross in one point, corresponding to ytterbium. This is ytterbia, which is the last one in the REO series, which crystallizes in more than one polymorphous form (C- and H-forms of REO), it is isomorphous with Y_2O_3. In the lutetia we can find C-form of REO only and, therefore, the only peritectic transformation $L + H \leftrightarrows C$ is the probable reaction with liquid phase. The linear dependences (Figs. 11 and 12) allow predicting the phase diagrams Nd_2O_3–Y_2O_3, Pr_2O_3–Y_2O_3 quite accurately. Based on that the lanthanide oxides of yttrium subgroup demonstrate full or almost full mutual solubility in yttria, the diagrams of the systems Yb_2O_3–Y_2O_3, Lu_2O_3–Y_2O_3, Tm_2O_3–Y_2O_3, Tb_2O_3–Y_2O_3, Ho_2O_3–Y_2O_3 simplified for prognosis and one can expect their topology might be similar the topology of earlier considered diagrams of the systems Dy_2O_3–Y_2O_3, Er_2O_3–Y_2O_3.

In the binary systems Ln_2O_3–Ln'_2O_3, formation of the chemical compound of ABO_3 with the perovskite-type

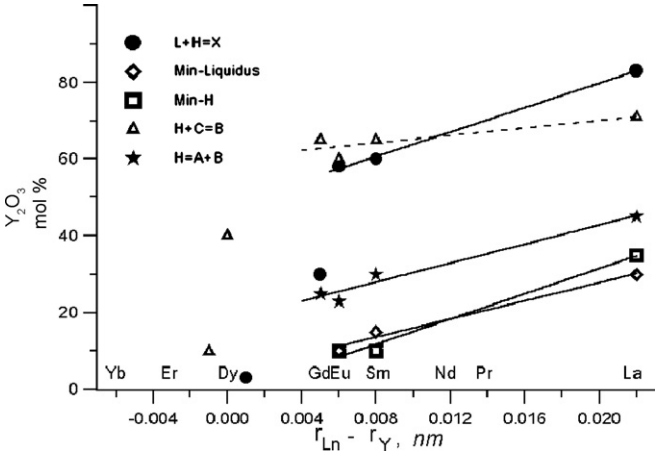

Fig. 12. Composition of invariant points in the binary systems Ln_2O_3–Y_2O_3 as a function of lanthanide ionic radius for cerium subgroup.

Table 7
Temperatures of formation/decay of the perovskite-type phase (ABO_3) in the systems Ln_2O_3-Ln'_2O_3[49]

A	B					
	Y	Ho	Er	Tm	Yb	Lu
La	1600	1700	1820	1955	2040	
Ce	–	–	–	1700	1900	2050
Pr	–	–	–	–	1500	1950
Nd	–	–	–	–	–	1300

structure was observed. The Goldsmith tolerance factor $t = (R_A + R_O)/\sqrt{2}(R_B + R_O)$ for the perovskite structure is in the limits $0.75 \leq t \leq 1.0$. This ratio is valid for the combination of lanthanides listed in Table 7 and in Fig. 13.

Apparently, the perovskite-type phase in the series Ln_2O_3–Y_2O_3 is stabilized in the lanthana-based systems. Meanwhile, the compound $LnYO_3$ was shown to be more stable when doped with zirconia or hafnia. Following tolerance factor, its value is growing when effective ion radius in the site B decreases due to substitution of these ions in part by smaller size ions of Zr^{4+}or Hf^{4+}. The dissolution of zirconia in large amount is impossible because of charge compensation. In Table 8 one can find estimated tolerance factors for doped perovskites.

The calculation of the tolerance factor for the perovskite-type phase, where cations are partially substituted by zirconium or hafnium ions, allows estimation of their stability or probability to be formed. Fig. 14 shows the changes which happen with minimal and maximal tolerance factors, when one of the cations is substituted. Obviously, the equiprobable substitution of cations gives the tolerance factor t, which is variable in the range between maximal and minimal values. The calculation revealed the difference in tolerance factor between zirconia and hafnia is minimal (in the third figure). The substitution of the praseodymium cations by zirconium or hafnium cations may result in stabilization of $PrYO_3$ on the "bottom threshold" of

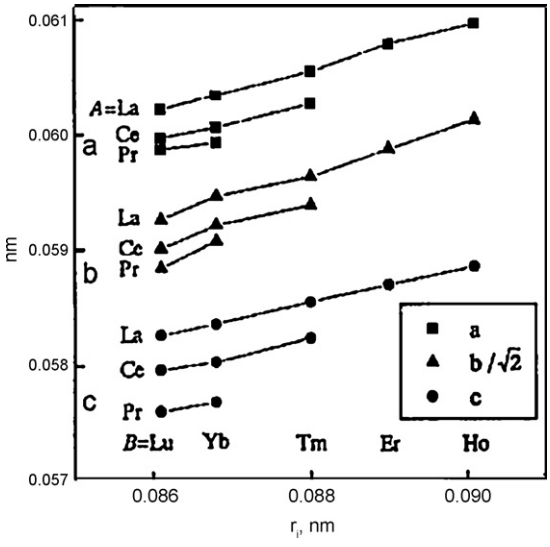

Fig. 13. Dependence of lattice parameter for the perovskite-type phase $LnYO_3$ versus lanthanide ionic radius.[49]

Table 8
Estimated stability of the perovskite-type phases $LnYO_3$ doped with ZrO_2

No.	Formula of doped perovskite phase/$t = (R_A + R_O)/\sqrt{2}(R_B + R_O)$	Comment
Stoichiometric phase $LnYO_3$		
1	Substitution in the site A: $Ln_{1-y}Zr_yYO_3$, $t_1 = \frac{(1-y)r_{Ln}+yr_{Zr}+r_o}{\sqrt{2}(r_Y+r_o)} \geq 0.843$	Ion Zr^{4+} substitutes ion Ln^{3+}. As $r_{Zr^{4+}} < r_{Ln^{3+}}$, than t_1 decreases with increase of ZrO_2 concentration
2	Substitution in the site B: $LnY_{1-y}Zr_yO_{3-(1/2y)}\square_{1+(1/2y)}$, $t_2 = \frac{r_{Ln}+r_O}{\sqrt{2}(yr_{Zr}+(1-y)r_Y+r_O)} \geq 0.843$	Ion Zr^{4+} substitutes ion Y^{3+}. As $r_{Y^{3+}} > r_{Zr^{4+}}$, than t_2 increases with increase of Y_2O_3 concentration

tolerance factor, 0.75, however, the equiprobable substitution of both praseodymium and yttrium ions, this factor becomes lower the formal threshold.

Thus, we suggest the perovskite-type phase $PrYO_3$ can appear in the ternary systems $HfO_2(ZrO_2)$–Y_2O_3–Pr_2O_3. The other REO do not form the phases of perovskite-type with yttria because of the spatial limitations. For the lanthanides with ionic radius smaller than one of yttrium ion (0.092 nm), the perovskite formation is very probable, and, actually, the existence of compounds ABO_3 (A = La–Nd, B = Dy–Lu) has been confirmed experimentally. For the binary rare-earth perovskites, the tolerance factor is going to be not less than 0.75.[49]

4. The regularities in constitution of liquidus, solidus surfaces in the systems $HfO_2(ZrO_2)$–Y_2O_3–Ln_2O_3

The above presented analysis of the high-temperature fields of the binary bounded systems and experimentally studied surfaces liquidus and solidus of the ternary systems, allow predicting constitutions of liquidus and solidus for unstudied systems in the series $HfO_2(ZrO_2)$–Y_2O_3–Ln_2O_3. The liquidus and solidus surfaces in the ternary systems are presented in Table 9 and Figs. 15–17.

The spatial factor is the determinative one for the constitution of these systems, in which the ionic type of chemical bonding prevails: the larger is the difference between ionic radii of components, the more complex is the topology of the phase diagram. Thus, the difference between ionic radii of zirconium and REO is smaller, than that for hafnium and the same REOs on 0.001 nm, but this is sufficient factor to get more complex liquidus for the system based on HfO_2 compared to ZrO_2-based one. The constitution of liquidus and solidus of the ternary system becomes simpler in the series from lanthanum to lutetium: for the REO of cerium subgroup the liquidus is more complex than that with REO of yttrium subgroup. In first case, many eutectic- and peritectic-type reactions have been revealed, but in the second one, invariant points have not been found. While the lanthanide ionic radius decreases, the number of invariant points decreases cymbately: from four points in case of praseodymium oxide to 0 for all REO heavier than terbia. If temperature of the peritectics and minima on liquidus surfaces in the binary systems Ln_2O_3–Y_2O_3 increases the temperature of ternary invariant points, or ternary minima of melting temperatures on liquidus surfaces increases cymbately as lanthanide's radii became closure. The number of primary crystallization fields on the liquidus surfaces and homogeneity fields on the solidus surfaces decreases from six (praseodymium) to three (lutetium). In the row from lanthanum to lutetium, the volume of the fluorite-type phase substantially increases. Two homogeneity fields of the fluorite solid solutions, inherent in several systems with REO of cerium subgroup, were found to increase in size while ionic radius of lanthanide decreases. The field of primary crystallization of X-phase gradually decreases and, in accordance with bounded binary systems Ln_2O_3–Y_2O_3, the

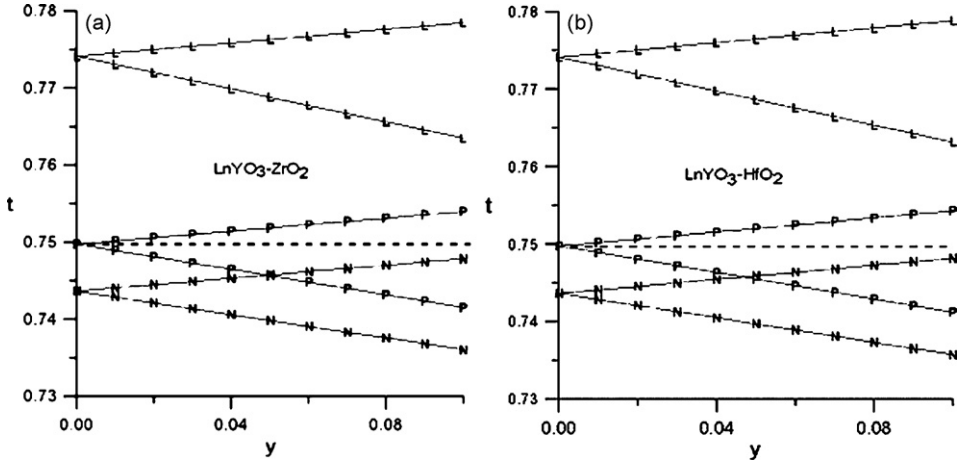

Fig. 14. Goldsmith tolerance factor (t) for the phase $LnYO_3$ doped with ZrO_2 (a) or with HfO_2 (b), vs. concentration of dopant (y).

Table 9
The coordinates of invariant points of the ternary systems $HfO_2(ZrO_2)$–Y_2O_3–Ln_2O_3

System	Composition, mol %		T,	Reaction	Composition, mol %		T,	Reaction	Composition, mol %		T,	Reaction
	ZrO_2	Y_2O_3	℃		ZrO_2	Y_2O_3	℃		ZrO_2	Y_2O_3	℃	
ZrO_2-Y_2O_3-La_2O_3	29	42	2250	L+F⇆Py+C	12	62	2200	L+H⇄X+C	24	24	2070	L+C⇄X+Py
ZrO_2-Y_2O_3-Pr_2O_3	22	38	2200	L+C⇆X+F	9	59	2330	L+H⇄X+C	-	-	-	
ZrO_2-Y_2O_3-Nd_2O_3	21	36	2220	L+C⇆X+F	10	54	2300	L+H⇄X+C	-	-	-	
ZrO_2-Y_2O_3-Sm_2O_3	20	50	2330	L+H⇆X+F	17	69	2360					
ZrO_2-Y_2O_3-Eu_2O_3	20	50	2340	L+C⇆H+F	20	40	2310	L+H⇄X+F	-	-	-	-
ZrO_2-Y_2O_3-Tb_2O_3	13	7	2230	L⇆X+C+H								
ZrO_2-Y_2O_3-Er_2O_3	12.5	41	2330	min, L⇆C+H	18	39	2350	min, L+F⇄C				
	HfO_2	Y_2O_3	T, °C	Reaction	HfO_2	Y_2O_3	T, °C	Reaction	HfO_2	Y_2O_3	T, °C	Reaction
HfO_2-Y_2O_3-La_2O_3	23	26.5	2040	L⇆X+Py+C	32	39	2230	L+F⇄Py+C	5	66	2170	L+H⇄X+C
HfO_2-Y_2O_3-Pr_2O_3	22	28	~2070	L⇆X+Py+C	30	38	~2240	L+F⇄Py+C	7	70	~2200	L+H⇄X+C
HfO_2-Y_2O_3-Nd_2O_3	20	35	~2200	L+F⇆C+X	-	-	-	-	10	62	~2300	L+H⇄X+C
HfO_2-Y_2O_3-Sm_2O_3	20	19	~2260	L+F⇆C+X	-	-	-	-	11	55	~2350	L+H⇄X+C
HfO_2-Y_2O_3-Eu_2O_3	19	36	2330	L+H⇆X+F	17	55.5	2360	L+C⇄H+F	-	-	-	-
HfO_2-Y_2O_3-Gd_2O_3	14	18	~2280	L+H⇆X+F	16	55	~2360	L+C⇄H+F	-	-	-	-
HfO_2-Y_2O_3-Tb_2O_3	6	14	2280	L⇆X+C+H	-	-	-	-	-	-	-	-
HfO_2-Y_2O_3-Er_2O_3	10.5	45.5	2360	min, L⇆C+H	15.5	49.5	2380	min, L+F⇄C	-	-	-	-
HfO_2-Y_2O_3-Tm_2O_3	11	40	2350	min, L⇆C+H	19.5	41	2400	min, L+F⇄C	-	-	-	-
HfO_2-Y_2O_3-Yb_2O_3	13	39	2370	min, L⇆C+H	20	52	2400	min, L+F⇄C				

Note: experimental data are marked with gray.

fields of primary crystallization of H- and C-phases increase at the expense of X-phase. Small homogeneity field of C-solid solutions in the systems from the beginning of series becomes dominating to the end, in particular, for the system with lutetium (Table 10).

In the series from lanthanum-based to lutetium-based system, the main feature of the phase transformations concerns increase of melting temperatures and phase transformations in the solid solutions and solid phase reactions. Thus, the difference in melting temperatures for the systems with lanthana is 720 °C (ZrO_2) and 760 °C (HfO_2) whereas for the systems with erbia this difference is 370 and 460 °C for ZrO_2 and HfO_2, respectively. This fact denotes the decrease of merging energy for the oxides when the solid solution is formed.

Comparing the ternary phase diagrams in the series ZrO_2–Y_2O_3–Ln_2O_3 and HfO_2–Y_2O_3–Ln_2O_3 we can find rich similarity between them. The differences in constitution originate from the properties of HfO_2 and ZrO_2. The general regularities of constitution of the considered ternary phase diagrams can be analyzed coming from the analysis of the boundary binary systems. It is right as the constitution of the ternary phase diagrams are determined by the constitution of the boundary binary systems. Obviously, the variable parameter is the ion radius of lanthanide (Ln^{3+}), which changes from 0.084 nm for Lu^{3+} to 0.114 nm for La^{3+}. It was found that the coordinates of invariant points in the series of diagrams ZrO_2–Ln_2O_3, HfO_2–Ln_2O_3, Y_2O_3–Ln_2O_3 linearly depend on ionic radii of lanthanides.

5. Stability intermediate phase pyrochlore-type in the systems $HfO_2(ZrO_2)$–Y_2O_3–Ln_2O_3

Phase equilibria with the pyrochlore phase (Py) are studied quite well in these ternary systems including REO of cerium subgroup. First, it was shown that in the systems $HfO_2(ZrO_2)$–Y_2O_3–Ln_2O_3 (Ln = La, Sm, Eu) the character of phase equilibria is determined by relatively high thermodynamic stability of the pyrochlore-type phase, which interacts with all phases in the systems. These properties allow identification of partially quasi-binary type for the sections $Ln_2Hf_2O_7(Ln_2Zr_2O_7)$–Y_2O_3. The sections are characterized by the restricted solid-state solubility of the components; moreover this solubility is quite substantial, as the solid solutions of Py and C-modification of REO possess lattices, derived from the fluorite-type solid solution with cubic symmetry. Second, it was revealed that the solubility of yttria affects the stability of the pyrochlore-type phase, and in the system with lanthana it changes the congruent type of melting for $La_2Zr_2O_7$ by incongruent. The pyrochlore-type phase forms solid solutions of substitution type with yttria and REO as a result of equiprobable substitution of cations in the sites Me^{3+} and Me^{4+} of the pyrochlore. The substitution of these cations by RE ion smaller than ion of La^{3+}

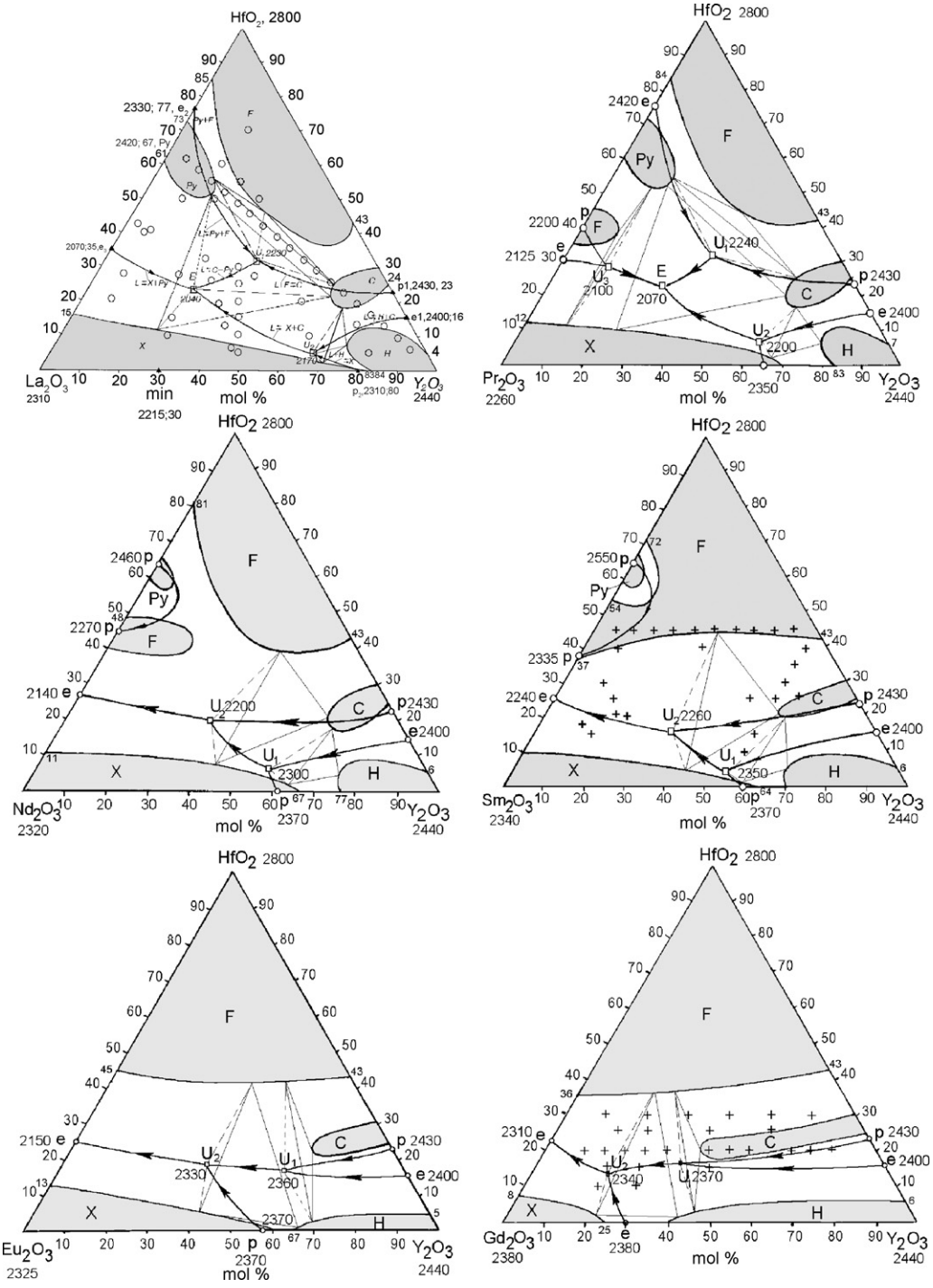

Fig. 15. Evolution of topology for the liquidus and solidus surfaces in the ternary systems HfO_2–Y_2O_3–Ln_2O_3 (Ln—REE of cerium subgroup) experiment (◯), calculation (+) and prognosis.

(0.114 nm) results in decrease of the ratio $R = (r_A/r_B)$ to critical Figs. 1 and 2 and, therefore, decreases the probability of ordering the pyrochlore phase. The same calculations were carried out for the pyrochlores doped with yttria in ternary systems. The substitution of ions in the non-stoichiometric pyrochlore is presented in Table 10.

Formation of solid solutions in the first variant case occurs if the compensation of the charge difference by oxygen vacancies, and in the second variant—without such compensation. Between these variants one can find many intermediate variants, because in the pyrochlore with excess of REO, and with excess of $ZrO_2(HfO_2)$, the yttrium ions may substitute any of these cations.

Thus, the selective substitution of ions Ln^{3+} in the pyrochlore, enriched with REO, is able to give the solid solution of $Ln_{2+x-y}Zr(Hf)_{2-x}Y_yO_{7-(x/2)}$. In the pyrochlore enriched with $ZrO_2(HfO_2)$ the selective substitution of Zr^{4+} (Hf^{4+}) by ions of yttrium provided the charge compensa-

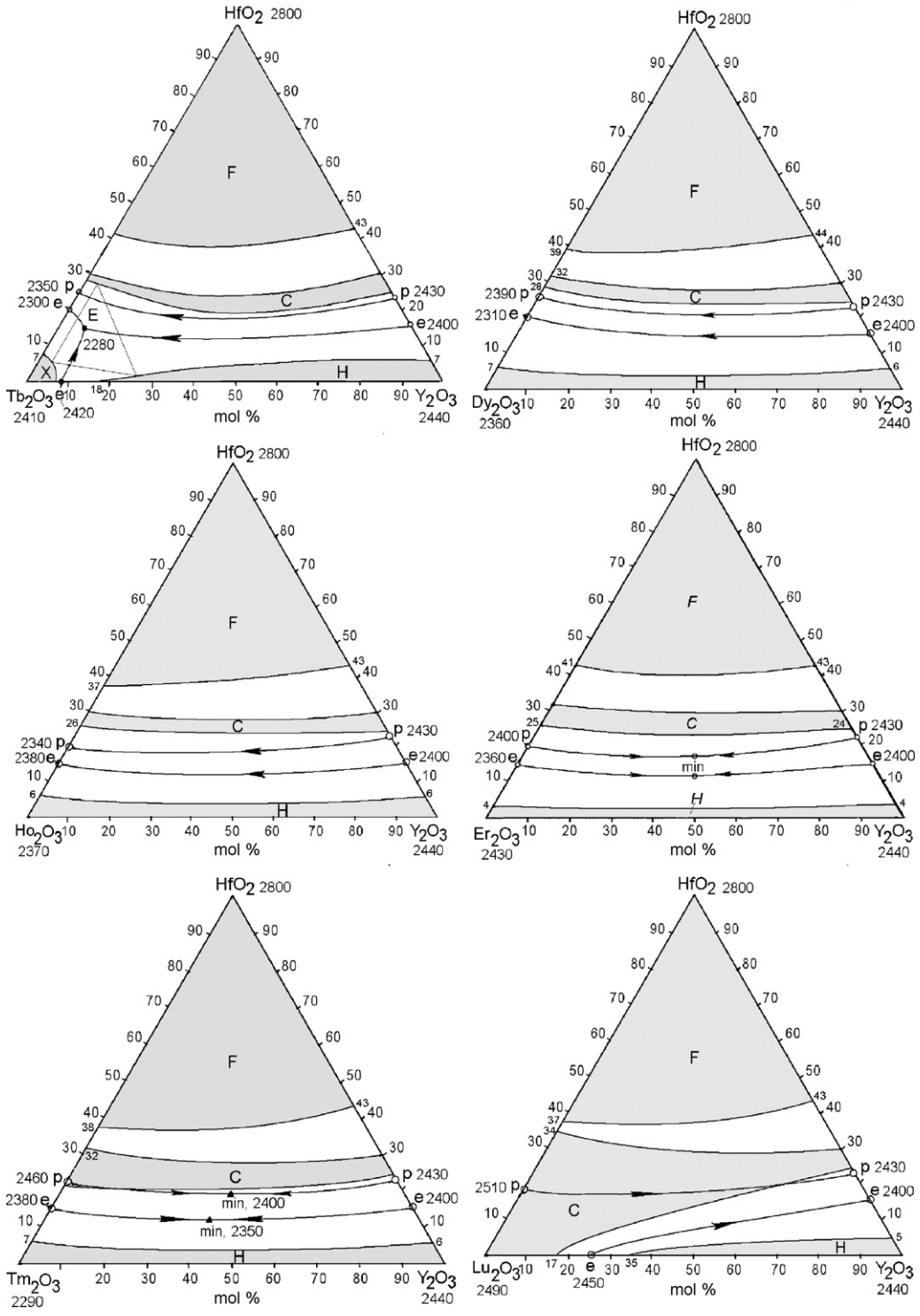

Fig. 16. Evolution of topology for the liquidus and solidus surfaces in the ternary systems HfO_2–Y_2O_3–Ln_2O_3 (Ln—REE of yttrium subgroup) experiment (◯), calculation (+) and prognosis.

tion in $Ln_{2-x}Zr(Hf)_{2+x-y}Y_yO_{(7+x)/(2-y)/2}$ The variants of solid solutions described above allow us to evaluate the size of homogeneity field for hafnates and zirconates of REO of cerium subgroup. The calculations of solubility were carried out, for undoped pyrochlores, taking into account, that the critical stability of the pyrochlore is defined by steric factor, i.e. the ratio of effective ionic radii in the sites A and B. Fig. 18 demonstrates decrease of yttria solubility in zirconates of lanthanides ($Ln_2Zr_2O_7$) with the decrease of ionic radius.

Obviously, the effective radii of both anion and cation in the pyrochlore-type phase change (increases for anions and decreases for cations) provided yttrium substitutes zirconium (hafnium) and lanthanide. As a sequence of this substitution the

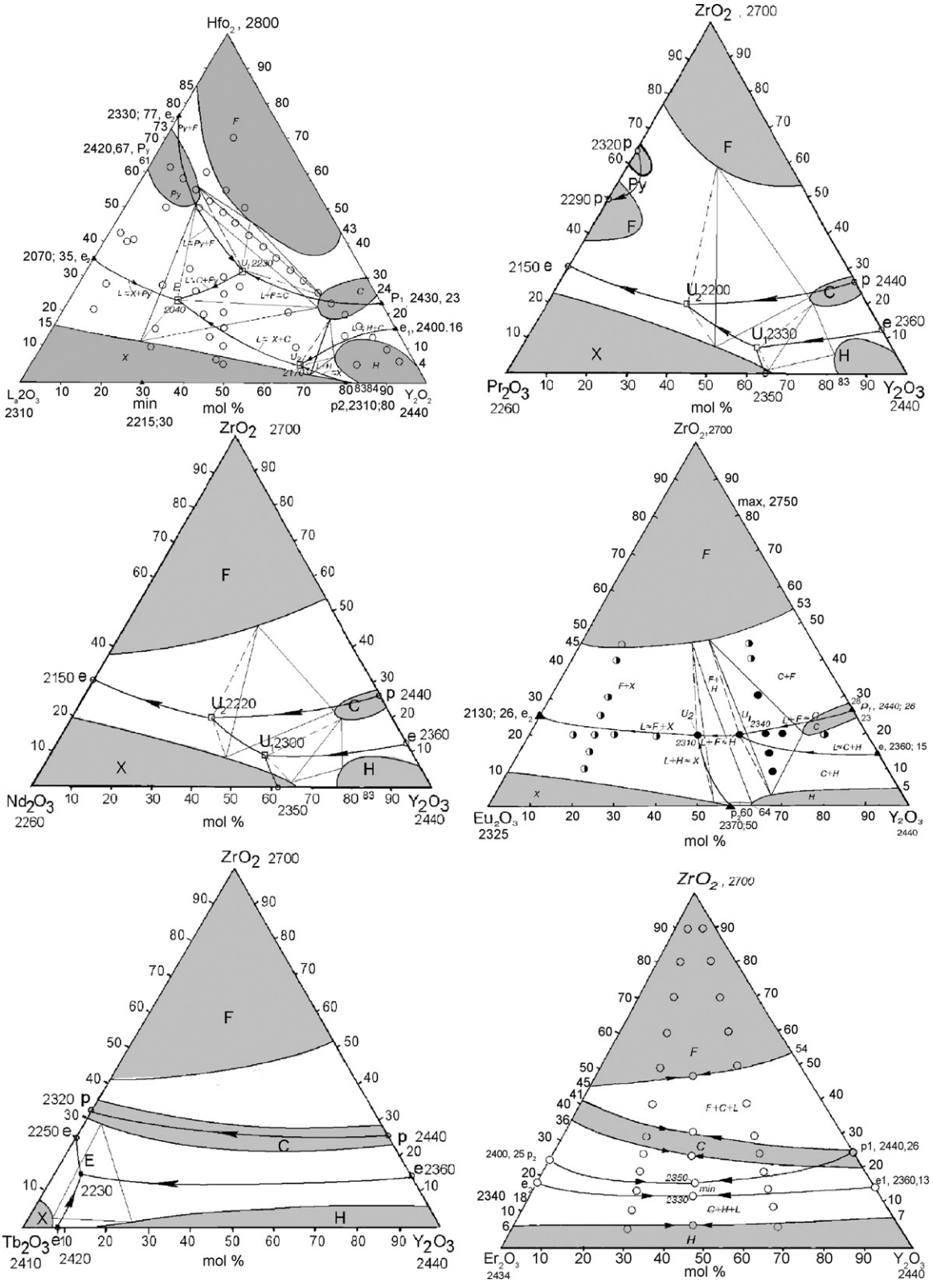

Fig. 17. Evolution of topology for the liquidus and solidus surfaces in the ternary systems ZrO_2–Y_2O_3–Ln_2O_3; (◯) experimental points; (◯) one-phase, (◑) two phase, (●) three-phase.

Table 10
Evaluation of stability for the pyrochlore-type phase being doped with yttria

No.	Formula of substituted pyrochlore/ratio $R = r_A/r_B$	Comment
Stoichiometric pyrochlore $Ln_2Zr_2O_7$		
1	Substitution in site A: $Ln_{2-y}Y_yZr_2O_7$, $R_1 = \frac{(2-y)r_{Ln}+yr_Y}{2r_{Zr}} \geq 1.2$	Ion Y^{3+} substitutes the ion Ln^{3+}. If $r_{Y^{3+}} < r_{Ln^{3+}}$, then R_1 decreases with increase of Y_2O_3 content
2	Substitution in site B: $Ln_2Zr_{2-y}Y_yO_{7-(1/2)y}\square_{1+(1/2)y}$, $R_2 = \frac{2r_{Ln}}{(2-y)r_{Zr}+yr_Y} \geq 1.2$	Ion Y^{3+} substitutes ion Zr^{4+}. If $r_{Y3+} > r_{Zr4+}$, then R_2 increases with increasing of Y_2O_3 amount
3	Substitution in sites A and B: $Ln_{2-x}Y_xZr_{2-y}Y_yO_{7-(y/2)}\square_{1+(y/2)}$, $R_3 = \frac{(2-x)r_{Ln}+xr_Y}{(2-y)r_{Zr}+yr_Y} \geq 1.2$	Ions Y^{3+} substitute the ions Ln^{3+} and Zr^{4+}. If $r_{Ln^{3+}} > r_{Y^{3+}} > r_{Zr^{4+}}$, then R_3 is able to increase, and decrease with concentration Y_2O_3
Pyrochlore phase with excess of lanthanide $Ln_2Zr_{2-x}Ln_xO_{7+(x/2)}\square_{1-(x/2)}$		
4	Substitution in site A: $Ln_{2-y}Y_yZr_{2-x}Ln_xO_{7+x/2}\square_{1-x/2}$, $R_4 = \frac{(2-y)r_{Ln}+yr_Y}{(2-x)r_{Zr}+xr_Y} \geq 1.2$	Ions Y^{3+} substitute ions Ln^{3+}. If $r_{Ln^{3+}} > r_{Y^{3+}}$, then R_4 decreases with increasing of Y_2O_3 concentration
5	Substitution in site B: $Ln_2Zr_{2-x-y}Ln_xY_yO_{7+(y/2)+(x/2)}\square_{1-(y/2)-(x/2)}$, $R_5 = \frac{2r_{Ln}}{(2-y-x)r_{Zr}+xr_{Ln}+yr_Y} \geq 1.2$	Ion Y^{3+} substitutes ion Zr^{4+}. If $r_{Y^{3+}} > r_{Zr^{4+}}$, then R_5 decreases with increasing of Y_2O_3 concentration
6	Substitution in site B: $Ln_2Zr_{2-x}Ln_{x-y}Y_yO_{7+(x-y)/2}\square_{1-(x-y)/2}$, $R_6 = \frac{2r_{Ln}}{(2-x)r_{Zr}+(x-y)r_{Ln}+yr_Y} \geq 1.2$	Ion Y^{3+} substitutes ion Ln^{3+} if $y<x$. If $r_{Y^{3+}} < r_{Ln^{3+}}$, then R_6 increases with increasing of Y_2O_3 concentration
Pyrochlore phase with excess of ZrO_2–$Ln_{2-x}Zr_xZr_2O_{7+(x/2)}\square_{1-(x/2)}$		
7	Substitution in site A: $Ln_{2-x-y}Zr_xY_yZr_2O_{7+(x/2)}\square_{1-(x/2)}$, $R_7 = \frac{(2-x-y)r_{Ln}+xr_{Zr}+yr_Y}{2r_{Zr}} \geq 1.2$	Ion Y^{3+} substitutes ion Ln^{3+}. If $r_{Y^{3+}} < r_{Ln^{3+}}$, then R_7 decreases with increasing of Y_2O_3 concentration
8	Substitution in site A: $Ln_{2-x}Zr_{x-y}Y_yZr_2O_{7+(x-y)/2}\square_{1-(x-y)/2}$, $R_8 = \frac{(2-x)r_{Ln}+(x-y)r_{Zr}+yr_Y}{2r_{Zr}} \geq 1.2$	Ion Y^{3+} substitutes ion Zr^{4+}. If $r_{Y^{3+}} > r_{Zr^{4+}}$, then R_8 increases with increasing of Y_2O_3 concentration Y_2O_3
9	Substitution in site B: $Ln_{2-x}Zr_xZr_{2-y}Y_yO_{7+(x/2-)y/2}\square_{1-(x/2)-(y/2)}$, $R_9 = \frac{(2-x)r_{Ln}+xr_{Zr}}{(2-y)r_{Zr}+yr_Y} \geq 1.2$	Ion Y^{3+} substitutes ion Zr^{4+}. If $r_{Y^{3+}} > r_{Zr^{4+}}$, then R_9 decreases with increasing of Y_2O_3 concentration

Note: r_{Zr}, r_{Ln}, r_Y, ion radii of zirconium, lanthanides and yttrium, respectively; $Ln_{2+x}Zr(Hf)_{2-x-y}Y_yO_{7-(y/2)-(x/2)}\square_{1+(y/2)+(x/2)}$, in case of the pyrochlore with excess of REO and as a result of substitution of $Zr^{4+}(Hf^{4+})$ by y ions of Y^{3+}; $Ln_{2-x-y}Zr(Hf)_{2+x}Y_yO_{7+(x/2)}\square_{1-(x/2)}$, in case of the pyrochlore with excess of $Zr(Hf)O_2$ when REO ions are substituted by y ions of Y^{3+}.

pyrochlore phase changes the congruent character of melting to incongruent.

Meanwhile, the experimental results obtained and the regularities found allow forecasting unknown systems of series $HfO_2(ZrO_2)$–Y_2O_3–Ln_2O_3 and larger series with various combinations of lanthanides, like ZrO_2–Ln'_2O_3–Ln''_2O_3. From the presented prognoses, one can find an evolution of topology for the liquidus and solidus surfaces with various relations of ions. We should mention the simplification of liquidus and solidus surfaces while difference between ionic radii decreases: 5–6 fields for the beginning of series and 3–2 fields for the end of one. If the ionic radii of lanthanide and yttrium are very close, the liquidus surface does not contain any invariant points.

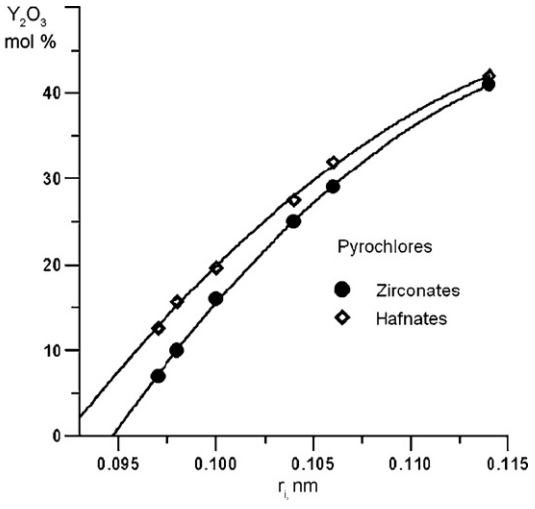

Fig. 18. Change of homogeneity fields for pyrochlore-type phases along the quasibinary sections $Ln_2Hf_2O_7$ ($Ln_2Zr_2O_7$)–Y_2O_3 by the data of calculations.

6. Conclusions

The main regularities of the phase diagrams in the series of binary and ternary systems based on zirconia (hafnia), yttria and lanthanide oxides have been revealed and extensively analyzed as a function of lanthanide ionic radius.

This study shows that temperatures and composition of eutectics, temperatures of intermediate phase stability, lattice parameters of solid solutions and others have changed linearly versus lanthanide's ionic radii.

The details of alloys crystallization in the systems $HfO_2(ZrO_2)$–Ln_2O_3, Y_2O_3–Ln_2O_3 and ternary $HfO_2(ZrO_2)$–Y_2O_3–Ln_2O_3 systems were studied and a prognoses of liquidus and solidus surfaces in unstudied systems were carried out.

References

1. Sayir, A. and Farmer, S. C., The effect of the microstructure on mechanical properties of directionally solidified $Al_2O_3/ZrO_2(Y_2O_3)$ eutectic. *Acta Mater.*, 2000, **48**, 4691–4697.
2. Lorca, J. L. and Orera, V. M., Directionally solidified eutectic ceramic oxides. *Prog. Mater. Sci.*, 2006, **51**, 711–809.
3. Paderno, Yu., Paderno, V. and Filippov, V., Crystal chemistry of eutectic growth of d- and f-transition metals borides. *Jpn. J. Appl. Phys. Ser.*, 1994, **10**, 190–193.
4. Wang, J., Li, H. P. and Stevens, R., Review. Hafnia and hafnia-toughened ceramics. *J. Mater. Sci.*, 1992, **27**(12), 5397–5430.
5. Stevens, R., *Introduction to Zirconia, Vol. 113*. Magnesium Electron Publication, 1986, p. 51.
6. Garvie, R. C., Hanning, R. H. and Pascal, R. T., Ceramic steel? *Nat. Lond.*, 1975, **258**, 703–704.
7. Hannink, R. H. J., Kelly, P. M. and Muddle, B. C., Transformation toughening in zirconia-containing ceramics. *J. Am. Ceram. Soc.*, 2000, **83**(3), 461–487.
8. Pandolfelli, V. C, Rainforth, M. and Stevens, R., Sintering and microstructural studies in the system ZrO_2–TiO_2–CeO_2. *J. Mater. Sci.*, 1990, **25**(4), 2233–2244.
9. Raj, R., Fundamental research in structural ceramics for service near 2000 °C. *J. Am. Ceram. Soc.*, 1993, **76**(9), 2147–2174.
10. Menezes, C. A. B., Lazar, D. R. R., Ussui, V., Lima, N. B. and Pashoal, J. O. A., Influence of dopant content on thermal degradation of ZrO_2–Ce_2O_3–Y_2O_3 Ceramics. *Key Eng. Mater., Adv. Powder Technol. II*, 2001, **189–191**, 192–197.
11. Muqtader, S. A., Sidhu, R. K., Negabhushan, E., Muzaffuraddin, K. and Samdani, S. G., Destabilization behaviour of ceria-stabilized tetragonal zirconia polycrystals by sodium sulphate and vanadium oxide melts. *J. Mater. Sci. Lett.*, 1993, **12**, 831–833.
12. Higashi, K., Sonoda, K., Ono, H., Sameshima, S. and Hirata, Y., Characterization of rare earth-doped ceria powders derived from oxalate co-precipitate. *Key Eng. Mater.*, 1999, **159/160**, 25–30.
13. Sakai, N., Hashimoto, T., Katsube, T., Yamaji, K., Negishi, H., Horita, T., Yokokawa, H., Xiong, Y. P., Nakagawa, M. and Takahashi, Y., Miscibility gap in CeO_2–ZrO_2–Y_2O_3 system as an electrode of solid oxide fuel cell. *Solid State Ionics*, 2001, **143**, 151–160.
14. Scofronic, G. L., Foltyn, S. R. and Muenchausen, R. E., Interfacial reaction products and film orientation in $YBa_2Cu_3O_7$-*x* on zirconia substrates with and without CeO_2 buffer layers. *J. Mater. Res.*, 1993, **8**(11), 2785–2798.
15. Schmid, H. K., Pennefather, R., Meriani, S. and Schmid, C., Redistribution of Ce and La during processing of Ce(La)–TZP/Al_2O_3 composites. *J. Eur. Ceram. Soc.*, 1992, **10**, 381–392.
16. Sun, Q., Zhao, Z., Chen, W., Qing, X., Xu, X. and Dai, F., Experimental study of stress-induced localized transformation plastic zones in tetragonal zirconia polycrystalline ceramics. *J. Am. Ceram. Soc.*, 1994, **77**(5), 1352–1356.
17. Wang, J., Zheng, X. H. and Stevens, R., Fabrication and microstructure-mechanical property relationships in Ce–TZPs. *J. Mater. Sci.*, 1992, **27**, 5348–5356.
18. Lee, J. H., Yoon, S. M., Kim, B. K., Kim, J., Lee, H.-W. and Song, H.-S., Electrical conductivity and defect structure of yttria-doped ceria-stabilized zirconia. *Solid State Ionics*, 2001, **144**, 175–184.
19. Yu, C. S. and Shetty, D. K., Transformation yielding, plasticity and crack-growth – resistance (R-curve) behaviour of CeO_2-TZP. *J Mater. Sci.*, 1990, **25**, 2025–2035.
20. Minh, N. Q., Ceramic fuel cells. *J. Am. Ceram. Soc.*, 1993, **76**(3), 563–588.
21. Minh, N. Q. and Takahashi, T., *Science and Technology of Ceramic Fuel Cells*. Elsevier, 1995, p. 151.
22. Meilicke and Haile, S., Ordered-transitions in gadolinium zirconate: a potential electrolyte material in solid oxide fuel cells. *Mater. Res. Soc. Proc.*, 1995, **393**, 55–60.
23. Yashima, M., Kakihana, M. and Yoshimura, M., Metastable-stable phase diagram in the zirconia-containing systems utilized in solid oxide fuel cell application. *Solid State Ionics*, 1996, **86–88**, 1131–1149.
24. Kharton, V. V., Naumovich, E. N. and Vecher, A. A., Research on the electrochemistry of oxygen ion conductors in the former Soviet Union. I. ZrO_2-based ceramic materials. *J. Solid State Electrochem.*, 1999, **3**, 61–81.
25. Kharton, V. V., Yaremchenko, A. A. and Naumovich, E. N., Research on the electrochemistry of oxygen ion conductors in the former Soviet Union. II. Perovskite-related oxides. *J. Solid State Electrochem.*, 1999, **3**, 303–326.
26. Kharton, V. V., Yaremchenko, A. A., Naumovich, E. N. and Marques, F. M. B., Research on the electrochemistry of oxygen ion conductors in the former Soviet Union. III. HfO_2-, CeO_2-, ThO_2-based oxides. *J. Solid State Electrochem.*, 2000, **4**, 243–266.
27. Kharton, V. V., Naumovich, E. N., Yaremchenko, A. A. and Marques, F. M. B., Research on the electrochemistry of oxygen ion conductors in the former Soviet Union. IV. Bismuth oxide-based ceramics. *J. Solid State Electrochem.*, 2001, **5**, 160–187.
28. Andrievski, R. A., State of the art and perspectives in the field of particulate nanostructured materials. *J. Mater. Sci. Technol.*, 1998, **14**(1), 97–103.
29. Duran, P., Villegas, M., Fernandez, I. F., Capel, F. and Moure, C., Theoretically dense and nanostructured ceramics by pressureless sintering of nanosized Y-TZP powders. *Mater. Sci. Eng.*, 1997, **A232**, 168–176.
30. Duran, P., Villegas, M., Fernandez, I. F., Capel, F. and Moure, C., Low temperature fully densified nanostructured Y-TZP ceramics. *J. Mater. Sci. Lett.*, 1996, **15**, 741–744.
31. Glushkova, V. B, Osiko, B., Sherbakova, L. G. *et al.*, Study of solid solutions in the system ZrO_2–Y_2O_3 as single crystals. *Izv. Akad. Nauk SSSR, Neorg. Mater.*, 1977, **13**, 2197–2201.
32. Glushkova, V. B., Koehler, E. K. and Sherbakova, L. G., The kinetics and mechanism of solid state reactions in the system of refractory oxides. *Sci. Ceram.*, 1970, **5**, 219–239.
33. Mayo, M. J., Processing of nanocrystalline ceramics from ultrafine particles. *Int. Mater. Rev.*, 1996, **41**(3), 85–115.
34. Chen, D.-J. and Mayo, M. J., Rapid rate sintering of nanocrystalline ZrO_2–3 mol% Y_2O_3. *J. Am. Ceram. Soc.*, 1996, **79**(2), 906–912.
35. Chen, D.-J. and Mayo, M. J., Densification and grain growth of ultrafine 3 mol% Y_2O_3–ZrO_2 ceramics. *Nanostructured Mater.*, 1993, **2**, 469–478.
36. Brossmann, U., Sodervall, U., Wurschum, R. and Schaefer, H.-E., O diffusion in nanocrystalline ZrO_2. In *Proceedings of the fourth International Conference on Nanostructured Materials, Vol. 462*, 1998. pp. 2–120.
37. Vassen, R. and Stoever, D., Conventional and new materials for thermal barrier coatings. Functional gradient materials and surface layers prepared by fine particles technology. In *NATO-ASI Series II: Mathematics, Physics and Chemistry, Vol. 16*, ed. M.-I. Baraton and I. Uvarova. Kluwer Academic Publishers, Dordrecht, 2001, pp. 199–218.
38. Cao, X. Q., Vassen, R., Jungen, W., Schwartz, S., Tietz, F. and Stoever, D., Thermal stability of lanthanum zirconate plasma-sprayed coating. *J. Am. Ceram. Soc.*, 2001, **84**(9), 2086– 2090.
39. Vassen, R., Cao, X. Q., Tietz, F., Basu, D. and Stoever, D., Zirconates as new materials for thermal barrier coatings. *J. Am. Ceram. Soc.*, 2000, **83**(8), 2023–2028.
40. Durazzo, M. and Riella, H. G., Effect of mixed powder homogeneity on the UO_2–Gd_2O_3 nuclear fuel sintering behavior. *Key Eng. Mater. Adv. Powder Technol. II*, 2001, **189–191**, 60–66.
41. Spink, D. R. and Schemel, J. H., Development of rare-earth pyrohafnates for power reactor control-rod materials. *J. Nucl. Mater.*, 1973, **49**(1), 1–9.
42. Ploetz, G. L., Ceramic materials for nuclear reactor controls and poison. *J. Am. Ceram. Soc. Bull.*, 1960, **39**(7), 362–365.
43. Spenke, H., Suitabillity of Europium as absorbing material in fast reactors. *Atomwirt. Atomotech.*, 1972, **17**(3), 161–164.
44. Leitten, C. F. and Beaver, R. I., Use of lanthanide oxide neutron absorbers in pressurized-water reactors. *Nucl. Appl.*, 1968, **4**(6), 399–417.
45. Curtis, C. E. and Tharp, A. G., Ceramic properties of europium oxide. *J. Am. Ceram. Soc.*, 1959, **42**(3), 151–156.
46. Suchomel, R. R. and Hunter, O., Effects of temperature and microstructure on the elastic properties of selected Eu_2O_3–HfO_2 compositions. *J. Am. Ceram. Soc.*, 1976, **59**(3–4), 149–152.
47. Chebotin, V. N., *Transport Phenomena in Ionic Crystals*. Ural University, Sverdlovsk, 1968, p. 181.

48. Weyl, A. and Janke, D., High temperature ionic conduction in multicomponenet solid oxide solutions based on zirconia. *J. Am. Ceram. Soc.*, 1997, **80**(4), 861–873.
49. Ito, K., Tezuka, K. and Hinatsu, Y., Preparation, magnetic susceptibility, and specific heat of interlantanide perovskites ABO_3 (A = La–Nd, B = Dy–Lu). *J. Solid State Chem.*, 2001, **157**, 173–197.
50. Maguire, E., Gharbage, B., Marques, F. M. B. and Labrincha, J. A., Cathode materials for intermediate temperature SOFCs. *Solid State Ionics*, 2000, **127**, 329–335.
51. Dusastre, V. and Kilner, J. A., Optimization of composite cathodes for intermediate temperature SOFC applications. *Solid State Ionics*, 1999, **126**, 163–174.
52. Ceder, G., Kohan, A. F., Aydinol, M. K., Tepesch, P. D. and Van der Ven, A., Thermodynamic of oxides with substitutional disorder: a microscopic model and evaluation of important energy contributions. *J. Am. Ceram. Soc.*, 1998, **81**(5), 517–525.
53. Yashima, M., Arashi, H., Kakihara, M. and Yoshimura, M., Determination of cubic–tetragonal phase boundary in $Zr_{1-x}Y_xO_{2-(x/2)}$ solid solutions by Raman spectroscopy. *J. Appl. Phys.*, 1993, **74**(12), 7603–7605.
54. Bogicevic, A., Wolverton, C., Crosbie, G. M. and Steehel, E. B., Defect ordering in aleovalently doped cubic zirconia from first principles. *Phys. Rev. B*, 2001, **64**, 1–14, P. 014106.
55. Corman, G. S. and Stubican, V. S., Phase equilibria and ionic conductivity in the system ZrO_2–Yb_2O_3–Y_2O_3. *J. Am. Ceram. Soc.*, 1985, **68**(4), 174–181.
56. Duh, Y.-G., Dai, H.-T. and Chiou, B.-S., Sintering, microstructure, hardness, and fracture toughness behavior of Y_2O_3–CeO_2–ZrO_2. *J. Am. Ceram. Soc.*, 1988, **71**(10), 813–819.
57. Glushkova, V. B., Kravchinskaya, M. V., Kuznetsov, A. K. and Tikhonov, P. A., *Hafnia and its Compounds with Rare-Earth Elements*. Nauka, Leningrad, 1984, p. 176.
58. Arseniev, P. A., Glushkova, V. B., Evdokimov, A. A., Keler, E. K., Kravtchenko, V. B., Kravchinskaya, M. V., Krzhihzanovskaya, V. A., Kuznetsov, A. K., Kurbanov, Kh. M., Potemkin, A. V., Tikhonov, P. A. and Zeitlin, M. N., Compounds of rare-earth elements. *Zirconates, Hafnates, Niobates, Tantalates Antimonates*. Nauka, Moskva, 1985, p. 261.
59. Arseniev, P. A., Kovba, L. M., Bagdasarov, Kh. S., Dzhurinskii, B. F., Potemkin, A. V., Pokrovski, B. I., Spiridonov, F. M., Antonov, V. A. and Ilyukhin, V. V., *Compounds of Rare-Earth Elements. Systems with Oxides of the I–III Groups of Elements*. Nauka, Moskva, 1983, p. 280.
60. Komissarova, L. N., Spiridonov, F. M. and Spitsin, V. I., On regular changes of composition and structure of compounds in the systems $HfO_2(ZrO_2)$–M_2O_3. *Dokl. Akad. Nauk SSSR*, 1968, **181**(4), 881–884.
61. Komissarova, L. N. and Spiridonov, F. M., On regularities of formation of intermediate compounds in the system $HfO_2(ZrO_2)$–M_2O_3. In *Proceedings of the 3rd All-Union Symposium on High-Temperature Chemistry of Silicates and Oxides*, 1972, pp. 39–43.
62. Tresvyatski, S. G., Lopato, L. M., Vishnevski, V. B., Godovannaya, I. N., Donets, I. G., Dubok, V. A., Zyrin, A. V., Lashneva, V. V., Lugovskaya, E. S., Pavlikov, V. N., Semenyuk, N. I., Tkachenko, V. D., Shevchenko, A. V. and Yurchenko, V. A., In *New Materials based on Oxides and Synthetic Fluosilicates*, ed. S. G. Tresvyatski. Naukova Dumka, Kiev, 1982. p. 204.
63. Rouanet, A., Contribution a l'etude des systemes zirconia—oxydes des lanthanides au voisinage de la fusion: Memoire de these. *Rev. Intern. Hautes Temper. Refract.*, 1971, **8**(2), 161–180.
64. Duran, P., Gonzalez, M., Moure, C., Jurado, J. R. and Pascual, C., A new tentative phase equilibrium diagram for the ZrO_2–CeO_2 system in air. *J. Mater. Sci.*, 1990, **25**, 5001–5006.
65. Duran, P., Caracteristiques des solutions solides de haute temperature entre l'oxide de hafnium et les oxydes de lanthanides. *Bull. Soc. Franc. Ceram. Vidrio*, 1974, **2**(102), 47–55.
66. Pascual, C. and Duran, P., Kinetics and mechanism of the solid state synthesis of fluorite in ZrO_2–Y_2O_3–Ln_2O_3 (Ln = Ce, Nd, Er). *J. Mater. Sci.*, 1982, **17**, 3431–3436.
67. Stubican, V. S., Recent progress in the field of ceramic systems. *Ceramics*, 1983, **36**(5), 46–57.
68. Stubican, V. S., Corman, G. S., Hellman, J. R. and Senft, G., Phase relationships in some ZrO_2 systems. In *Advanced in Ceramics, Vol. 12*, ed. A. V. Heuer and L. W. Hobbs. The American Ceramic Society, Columbus, 1984, pp. 96–106.
69. Coutures, J., Sibieude, F. and Foex, M., Etude a Haute Temperature des Systems Formes par les sesquioxides de Lanthane Avec les Sesquioxydes de Lanthanides II. Influence de la Trempe sur la Nature des Phases Obtenues a la Temperature Ambiante. *J. Solid State Chem.*, 1976, **17**(4), 377–384.
70. Coutures, J., Rouanet, A., Verges, R. and Foex, M., Etude a Haute Temperature des Systems Formes par le Sesquioxyde de Lanthane et les Sesquioxydes de Lanthanides. I. Diagrammes de Phases ($1400\,C < T < T$ Liquide). *J. Solid State Chem.*, 1976, **17**(1/2), 172–182.
71. Piconi, C. and Maccauro, G., Zirconia as a ceramic biomaterial. *Biomaterials*, 1999, **20**, 1–25.
72. Zhu, D. and Miller, R., Development of advanced low conductivity thermal barrier coatings. *Int. J. Appl. Ceram. Technol.*, 2004, **1**(1), 86–94.
73. Yong, D., Masatomo, Y., Toshiaki, K., Masato, K. and Yoshimura, M., Measurement and calculation of the ZrO_2–CeO_2–$LaO_{1.5}$ phase diagram. *Calphad*, 1996, **20**(1), 95–108.
74. Li, L., Van Der Biest, O., Wang, P. L., Vleugels, J., Chen, W. W. and Huang, S. G., Estimation of the phase diagram for the ZrO_2–Y_2O_3–CeO_2 system. *J. Eur. Ceram. Soc.*, 2001, **21**, 2903–2910.
75. Park, S. Y., Kim, J. H., Kim, M. C, Song, H. S. and Park, C. G., Microscopic observation of degradation behavior in yttria and ceria stabilized zirconia thermal barrier coatings under hot corrosion. *Surf. Coatings Technol.*, 2005, **190**, 357–365.
76. Rey, F. Q. and Muccillo, E. N. S., Lattice parameters of yttria-doped ceria solid electrolytes. *J. Eur. Ceram. Soc.*, 2004, **24**, 1287–1290.
77. Idemitsu, K., Arima, T., Inagaki, Y., Torikai, S. and Pouchon, M. A., Manufacturing of zirconia microspheres doped with erbia, yttria and ceria by internal gelation process as a part of a cermets fuel. *J. Nucl. Mater.*, 2003, **319**, 31–36.
78. Ishihara, T., Shibayama, T., Ishikawa, S., Hosoi, K., Nishiguchi, H. and Takita, Y., Novel fast oxide ion conductor and application for the electrolyte of solid oxide fuel cell. *J. Eur. Ceram. Soc.*, 2004, **24**, 1329–1335.
79. Haering, C., Roosen, A. and Schichl, H., Degradation of the electrical conductivity in stabilised zirconia systems. Part I. Yttria-stabilised zirconia. *Solid State Ionics*, 2005, **176**, 253–259.
80. Chevalier, J., Deville, S., Münch, E., Jullian, R. and Lair, F., Critical effect of cubic phase on aging in 3 mol% yttria-stabilized zirconia ceramics for hip replacement prosthesis. *Biomaterials*, 2004, **25**, 5539–5545.
81. Mangalaraja, R. V., Chandrasekhar, B. K. and Manohar, P., Effect of ceria on the physical, mechanical and thermal properties of yttria stabilized zirconia toughened alumina. *Mater. Sci. Eng.*, 2003, **A343**, 71–75.
82. Elyassi, B., Rajabbeigi, N., Khodadadi, A., Mohajerzadeh, S. S. and Sahimi, M., An yttria-doped ceria-based oxygen sensor with solid-state reference. *Sens. Actuators*, 2004, **B103**, 178–183.
83. Lopato, L. M., Shevchenko, A. V. and Kuschevski, A. E., Study of the high-refractory oxide systems. *Powder Metall.*, 1972, **1**, 88–92.
84. Stegniy, A. I., Shevchenko, A. V., Lopato, L. M., Ruban, A. K., Dvernyakov, V. S. and Pasichnyy, V. V., Thermal analysis of oxides using solar heat. *Dokl. Akad. Nauk USSR*, 1979, **Ser. A**(6), 484–489.
85. Shevchenko, A. V., Tkachenko, V. D., Lopato, L. M., Ruban, A. K. and Pasichnyy, V. V., Techniques for measurement of phase transition temperatures using solar heating. *Powder Metall.*, 1986, **1**, 91–94.
86. Frolov, A. R., Andrievskaya, E. R. and Lopato, L. M., The application of concentrated light radiation for development of technological methods of the high-temperature melting of oxide compounds. In *Proceedings of the International Conference Science for Materials in the Frontier of Centuries: Advantages and Challenges, Vol. 1*, 2002, pp. 312–313.
87. Andrievskaya, E. R., *Phase Relations and Nanocrystalline Alloys in the Ternary Systems $ZrO_2(HfO_2)$–Y_2O_3–$La_2O_3(Eu_2O_3, Er_2O_3)$. Functional Gradient Materials and Surface Layers Prepared by Fine Particles Technology, Vol. 16*. Kluwer Academic Publishers, London, 2001, pp. 305–312.
88. Lefevre, J., Some structural modifications of fluorite-type phase in the systems based on ZrO_2 or HfO_2. *Annu. Chim.*, 1963, **8**(1–2), 254–256.

89. Komissarova, L. N., Van, G.-S., Spitsin, V. I. and Simanov, B. P., The system HfO_2–La_2O_3. *Zh. Neorg. Khim.*, 1964, **9**(3), 694–697.
90. Komissarova, L. N., Van, G.-S., Spitsin, V. I. and Simanov, B. P., On reaction of hafnium hydroxide with hydroxides of yttrium, lanthanum, neodymium and ytterbium. *Izv. Akad. Nauk SSSR Ser. Chem.*, 1965, **1**, 3–11.
91. Duran, P., Phase relationships in the systems HfO_2–La_2O_3 and HfO_2–Nd_2O_3. *Ceram. Intern.*, 1975, **1**(1), 10–13.
92. In I. V. Grebenshikov (Ed.), *Diagrams of State in the High-Melting Oxide Systems. Companion. Issue 5. Binary Systems. Part 1*. Institute of Chemistry Silicate, Nauka, Leningrad, 1985, p. 284.
93. Portnoi, K. I., Timofeeva, N. I., Salibekov, S. E. and Romanovich, I. V., Synthesis and study of properties of complex oxygen-containing compounds of REE and hafnium. *Izv. Akad. Nauk SSSR Neorg. Mater.*, 1970, **6**(1), 91–95.
94. Portnoi, K. I., Salibekov, S. E. and Timofeeva, N. I., Synthesis of hafnates of REE and study of their properties. *High-Temperature Chemistry of Silicates and Oxides*. Nauka, Leningrad, 1972, pp. 43–45.
95. Aldebert, P., Badie, J. M., Traverse, J. P., Buevoz, J. L. and Roult, G., Application d'un dispositif de diffraction des neutrons a haute temperature a l'etude d'oxydes refractraires. *Rev. Intern. Hautes Temp. Refract.*, 1975, **12**(1–4), 307–319.
96. Shevchenko, A. V. and Lopato, L. M., Influence of hafnium dioxide on lanthanide oxide polymorphism. *Dokl. Akad. Nauk USSR Ser. B*, 1975, **8**, 737–739.
97. Karyakina, E. L., Zoz, E. I., Gavrish, A. M. and Gul'ko, N. V., Some crystallochemical and thermalphysic characteristics of lanthanum zirconates and hafnates. *Zh. Neorg. Khim.*, 1978, **23**(12), 3202–3205.
98. Shevchenko, A. V., Lopato, L. M. and Ruban, A. K., Study of reactions in the system hafnia–lanthanum hafnate. *Dokl. Akad. Nauk USSR Ser. B*, 1976, **10**, 925–928.
99. Le, T. C., Interaction of hafnia with oxides of some light rare-earth elements. PhD Thesis, Moscow State University, Moskow, 1977.
100. Shevchenko, A. V. and Lopato, L. M., Influence of lanthanide oxides of cerium subgroup on hafnia polymorphism. *Dokl. Akad. Nauk USSR Ser. B*, 1977, **8**, 718–721.
101. Zoz, E. I., Gavrish, A. M. and Gul'ko, N. V., Phase formation in the systems ZrO_2 (HfO_2)–La_2O_3. *Izv. Akad. Nauk SSSR Neorg. Mater.*, 1978, **14**(1), 109–111.
102. Shevchenko, A. V. and Lopato, L. M., The systems HfO_2-rare earth oxides in the field rich with REO. *Izv. Akad. Nauk SSSR Neorg. Mater.*, 1982, **18**(11), 1842–1846.
103. Shevchenko, A. V., Lopato, L. M. and Zaitseva, Z. A., Interaction of HfO_2 with lanthana, praseodymia and neodymia at high temperatures. *Izv. Akad. Nauk SSSR Neorg. Mater.*, 1984, **20**(9), 1530–1534.
104. Shevchenko, A. V., Lopato, L. M., Stegnii, A. I., Ruban, A. K., Dvernyakov, V. S. and Pasichnyy, V. V., Liquidus of the systems hafnia—rare earth oxides in the field rich with HfO_2. *Izv. Akad. Nauk SSSR Neorg. Mater.*, 1981, **17**(6), 1022–1026.
105. Kuznetsov, A. K., Kravchinskaya, M. V. and Tikhonov, P. A., The system HfO_2–Pr_2O_3. *Zh. Neorg. Khim.*, 1976, **21**(5), 1317–1325.
106. Spiridonov, F. M., Le Thnong, C. and Komissarova, L. N., On interaction of hafnium dioxide with light rare-earth oxides. In *Proceedings of the 5th All-Union Symposium on Physicochemical Analysis*, 1976, pp. 56–57.
107. Kravchinskaya, M. V., Tikhonov, P. A., Kuznetsov, A. K. and Ganits, F., Phase relations in the system HfO_2–$PrO_{1.5}$–$DyO_{1.5}$. *Dokl. Akad. Nauk SSSR*, 1978, **238**, 583–585.
108. Kravchinskaya, M. V., Kuznetsov, A. K., Tikhonov, P. A. and Koehler, E., Phase diagrams of the systems HfO_2–Pr_2O_3 and Dy_2O_3–Pr_2O_3. *Ceram. Intern.*, 1978, **4**, 14–16.
109. Tikhonov, P. A., Sazonova, L. V., Glushkova, V. B. and Kravchinskaya, M. V., Solid solutions in the systems HfO_2–Nd_2O_3 (Pr_2O_3, Tb_2O_3) with mixed conductivity. *Zh Phys. Khim.*, 1980, **54**, 1967–1970.
110. Glushkova, V. B., Sazonova, L. V. and Ganits, F., Study of the system Nd_2O_3–HfO_2. *Izv. Akad. Nauk SSSR Neorg. Mater.*, 1978, **14**(11), 2096–2101.
111. Gavrish, A. M., Zoz, E. I., Gul'ko, N. V. and Soloviova, A. E., Study of solid solutions in the system HfO_2–CeO_2. *Izv. Akad. Nauk SSSR Neorg. Mater.*, 1975, **11**(4), 668–670.
112. Spiridonov, F. M., Chyong, L.-T. and Komissarova, L. N., The system HfO_2–CeO_2. *Zh. Neorg. Khim.*, 1977, **22**(2), 588–589.
113. Zoz, E. I., Yeliseeva, G. G. and Fomichev, E. N., Investigation of structure and dilatation properties of solid solutions in the system HfO_2–CeO_2. *Zh. Neorg. Khim.*, 1979, **24**(12), 3198–3200.
114. Shevchenko, A. V., Maister, I. M., Lopato, L. M. and Zaitseva, Z. A., Phase reactions in the system of HfO_2 with CeO_2 at high temperatures. *Izv. Akad. Nauk SSSR Neorg. Mater.*, 1983, **19**(5), 843–844.
115. Hirotaka, F., Masatomo, Y., Satoshi, S. and Masato, K., Internal distortion in ceria-doped hafnia solid solutions: high-resolution X-ray diffraction and Raman scattering. *J. Am. Phys. Soc., Phys. Rev. B*, 2001, **64**(13), 13104–13108.
116. Andrievskaya, E. R. and Lopato, L. M., Phase interactions and properties in the systems $HfO_2(ZrO_2)$–Y_2O_3–Ln_2O_3. In *Proceedings of the International Conference Advanced ceramics for third millennium*, 2001, p. 38.
117. Andrievskaya, E. R., Red'ko, V. P. and Lopato, L. M., Reactions of cerium oxide with hafnium, zirconium and yttrium oxides at 1500 °C. *Powder Metall.*, 2001, **7/8**, 109–118.
118. Andrievskaya, E. R., Red'ko, V. P. and Lopato L. M., Phase equilibria in the systems $ZrO_2(HfO_2)$–Y_2O_3–CeO_2. In Proceedings of the 10th International Conference on Modern Materials and Technologies. World Ceramic Congress and Forum on New Materials, Florence, Italy, July 2002, In P. Vincenzini (ed.), Techna Srl., 2003, Part A, pp. 49–56.
119. Andrievskaya, E. R., Red'ko, V. P. and Lopato, L. M., Phase relations and properties in the system HfO_2–Y_2O_3–CeO_2. In Proceedings of the International Conference Deformation and Fracture in Structural PM Materials, Stará Lesná, Slovakia, 2002, *Vol. 2*, IMR-SAS, Košice, 2002, pp. 110–114.
120. Duran, P., The system hafnia–samaria. *J. Am. Ceram. Soc.*, 1979, **62**(1/2), 9–12.
121. Isupova, E. N., Glushkova, V. B. and Keler, E. K., Study of the system HfO_2–Sm_2O_3 in solid state of the field rich with hafnia. *Izv. Akad. Nauk SSSR Neorg. Mater.*, 1968, **4**(3), 399–405.
122. Shevchenko, A. V., Lopato, L. M. and Nazarenko, L. V., The systems of HfO_2 with oxides of samarium, gadolinium, terbium and dysprosium at high temperatures. *Izv. Akad. Nauk SSSR Neorg. Mater.*, 1984, **20**(11), 1862–1866.
123. Perova, E. B., Study of Reactions between hafnium dioxide and oxides of some rare-earth elements, PhD Thesis, Moscow State University, Moskow, 1972.
124. Klee, W. E. and Weitz, G., Infrared spectra of ordered and disordered pyrochlore-type compounds in the series $RE_2Ti_2O_7$, $RE_2Zr_2O_7$ and $RE_2Hf_2O_7$. *J. Inorg. And Nucl. Chem.*, 1969, **31**(8), 2367–2372.
125. Delamarre, C., Contribution a l'etude de quelques systems HfO_2–MO. *Rev. Intern. Hautes Temp. Refract.*, 1972, **9**, 209–224.
126. Zhidovinova, S. V., Kotlyar, A. G., Strekalovski, V. N. and Pal'guev, S. F., Crystallochemical characteristics and electric conductivity of solid solutions based on REO and HfO_2. In *Proceedings of the Institute of Electrochemistry UNC Akad. Nauk SSSR, Vol. 18*, 1972, pp. 148–150.
127. Zhidovinova, S. V., Comparative characteristics of the phase formation on reaction between REE oxides and yttria with oxides of zirconium and hafnium, PhD, Thesis, Institute of Electrochemistry UNC Akad. Nauk SSSR, Sverdlovsk, 1974.
128. Zhidovinova, S. V., Strekalovski, V. N. and Pal'guev, S. F., Phase constitution of the system HfO_2–Eu_2O_3 in the field rich with HfO_2. *Izv. Akad. Nauk SSSR Neorg. Mater.*, 1975, **11**(10), 1809–1811.
129. Scheidecker, R. W., Wilder, D. R. and Moeller, H., The system HfO_2–Eu_2O_3. *J. Am. Ceram. Soc.*, 1977, **60**(11/12), 501–504.
130. Shevchenko, A. V., Lopato, L. M., Stegnii, A. I., Maister, I. M., Dvernyakov, V. S. and Pasichnyy, V. V., Liquidus in the systems HfO_2–TiO_2, ZrO_2–TiO_2, HfO_2–Eu_2O_3. *Dokl. Akad. Nauk USSR Ser. A*, 1979, **7**, 585–588.
131. Zoz, E. I., Fomichev, E. N., Kalashnik, A. A. and Yeliseeva, G. G., On structure and properties of REE zirconates and hafnates. *Zh. Neorg. Khim.*, 1982, **27**(1), 95–99.

132. Isupova, E. N., Glushkova, V. B. and Keler, E. K., Study of the system Gd_2O_3–HfO_2 in the hafnium dioxide rich field. *Izv. Akad.Nauk SSSR Neorg. Mater.*, 1968, **4**(10), 1732–1737.
133. Spiridonov, F. I., Stepanov, V. A., Komissarova, L. N. and Spitsyn, V. I., The binary System HfO_2–Gd_2O_3. *J. Less Commun. Metals*, 1968, **14**(5), 435–443.
134. Duran, P., Phase relationships in the hafnia–gadolinia system. *Ceramurgia Intern.*, 1977, **3**(4), 137–140.
135. Lopato, L. M., Andrievskaya, E. R., Shevchenko, A. V. and Red'ko, V. P., The interaction of europium oxide with hafnia, zirconia and yttria. In *Proceedings of the 4th International Workshop on Chemistry and Technology of High-Temperature Superconductors*, 1995, p. 91.
136. Andrievskaya, E. R. and Lopato, L. M., The systems $ZrO_2(HfO_2)$–Eu_2O_3. In *Proceedings International Conference Deformation and Fracture in Structural PM Materials with a Workshop on their Application*, 1996, pp. 296–301.
137. Andrievskaya, E. R., Lopato, L. M., Red'ko, V. P., Frolov, A. A. and Shevchenko, A. V., Characterization and properties phases in the HfO_2–Y_2O_3–Eu_2O_3 ternary system. In *Proceedings of the 5th International School Phase Diagrams in Materials Science, 1996*, 1996, pp. 14–15.
138. Andrievskaya, E. R. and Lopato, L. M., Phase transformations in the ternary systems $HfO_2(ZrO_2)$–Y_2O_3–Eu_2O_3. Key engineering materials, Trans Tech Publications, Switzerland, 1997, 132–136, 1782–1785.
139. Andrievskaya, E. R., Lopato, L. M., Shevchenko, A. V. and Smirnov, V. P., Phase interaction in the system HfO_2–Eu_2O_3. *Izv. RAN Neorg. Mater.*, 1997, **33**(7), 835–838.
140. Perova, E. B., Spiridonov, F. M. and Komissarova, L. N., Phase equilibria in the system HfO_2–Dy_2O_3. *Izv. Akad. Nauk SSSR Neorg. Mater.*, 1972, **8**(10), 1878–1880.
141. Gailler, M., Deportes, Ch., Robert, G. and Vitter, G., Etude structure dans le system HfO_2–Y_2O_3. *Rev. Intern. Haute Temp. Refract.*, 1967, **4**, 269–271.
142. Spiridonov, F. M., Komissarova, L. N., Kocharov, A. G. and Spitsin, V. I., The system HfO_2–Y_2O_3. *Zh. Neorg. Khim.*, 1969, **14**(9), 2535–2540.
143. Isupova, E. N., Glushkova, V. B. and Keler, E. K., Study of the system Y_2O_3–HfO_2 in the field rich with hafnium oxide. *Izv. Akad. Nauk SSSR Neorg. Mater.*, 1969, **5**(11), 1948–1952.
144. Duclot, M., Vicat, I. and Deportes, Ch., Mise en evidence et etude de la phase ordonnee $Y_2Hf_2O_7$ dans le systeme HfO_2–Y_2O_3. *J. Solid State Chem.*, 1970, **2**(2), 236–249.
145. Glazachev, V. S., Lukin, E. S., Balashev, V. A. and Borovkova, L. B., The mechanism of formation for solid solutions in the systems Y_2O_3–HfO_2 and Y_2O_3–ZrO_2. *Izv. Akad. Nauk SSSR, Neorg. Mater.*, 1977, **13**, 1814–1816.
146. Portnoi, K. I., Romanovich, I. V. and Timofeeva, E. N., Study of interaction between hafnium dioxide and yttrium oxide. *Izv. Akad. Nauk SSSR Neorg. Mater.*, 1971, **11**(5), 888–889.
147. Sukharevski, B. Ya., Gavrish, A. M., Zoz, E. I. and Soloviova, A. E., Determination of the boundaries for the fluorite solid solutions of Y_2O_3 in the HfO_2. *Dokl. Akad. Nauk SSSR*, 1973, **208**(5), 1086–1088.
148. Gavrish, A. M., Sukharevski, B. Ya., Zoz, E. I. and Soloviova, A. E., X-ray study of the phase relations in the systems HfO_2–CaO and HfO_2–Y_2O_3. *Izv. Akad. Nauk SSSR Neorg. Mater.*, 1973, **9**(2), 260–264.
149. Duran, P., Estadio de systema binarico HfO_2–Y_2O_3. *Bull. Soc. Esp. Ceram. Vidrio*, 1973, **12**(6), 341–346.
150. Stacy, D. W. and Widler, R. R., The yttria–hafnia system. *J. Am. Ceram. Soc.*, 1975, **58**(7–8), 285–288.
151. Volchenkova, Z. S., Zubankova, D. S. and Gorelov, V. P., Crystalline and defect structure of the samples in the system HfO_2–Y_2O_3. In *Proceedings Institute of Electrochemistry UNC Akad. Nauk SSSR, Vol. 24*, 1976, pp. 66–71.
152. Zubankova, D. S. and Volchenkova, Z. S., Character of conductivity in the system HfO_2–Y_2O_3. In *Proceedings Institute of Electrochemistry UNC Akad. Nauk SSSR, Vol. 23*, 1976, pp. 89–93.
153. Volchenkova, Z. S. and Zubankova, D. S., Phase composition and electric conductivity in the system HfO_2–Y_2O_3. In *Proceedings Institute of Electrochemistry UNC Akad. Nauk SSSR, Vol. 23*, 1976, pp. 83–88.
154. Shevchenko, A. V., Lopato, L. M. and Kir'yakova, I. E., The reactions of HfO_2 with Y_2O_3, Ho_2O_3, Er_2O_3, Tm_2O_3, Yb_2O_3 and Lu_2O_3 at high temperatures. *Izv. Akad. Nauk SSSR Neorg. Mater.*, 1984, **20**(12), 1991–1996.
155. Shevchenko, A. V., Lopato, L. M., Obolonchik, T. V., Tkachenko, V. D. and Nazarenko, L. V., The liquidus surface in the HfO_2–ZrO_2–Y_2O_3 system. *Izv. Akad. Nauk SSSR Neorg. Mater.*, 1987, **23**(4), 452–456.
156. Trubelja, M. F. and Stubican, V. S., Phase equilibria and ordering in the system zirconia–hafnia–yttria. *J. Am. Ceram. Soc.*, 1988, **71**(8), 662–666.
157. Belyaev, I. N. and Artamonova, S. M., Some physicochemical properties of co-precipitated hydroxides of holmium with zirconium and holmium with hafnium. *Izv. Akad. Nauk SSSR Neorg. Mater.*, 1969, **5**, 93–96.
158. Glushkova, V. B., Hanic, F. and Sazonova, L. V., Lattice parameters of cubic solid solutions in the systems uR_2O_3–(1-u)MO_3. *Ceram. Intern.*, 1978, **4**(4), 176–178.
159. Spiridonov, F. M. and Komissarova, L. N., The system HfO_2–Er_2O_3. *Zh. Neorg. Khim.*, 1970, **15**(3), 875–878.
160. Wilder, D. R., Buckley, G. D., Stacy, D. W. and Johnstone, J. K., Characterization and control of the destructive crystalline transformation in hafnium oxide. *Colloq. Intern. Centre Nat. Res. Sci.*, 1972, **205**, 335–345.
161. Duran, P., Pascual, C., Coutures, J. P. and Skaggs, S. R., Phase relations and ordering in the system erbia–hafnia. *J. Am. Ceram. Soc.*, 1983, **66**(2), 101–106.
162. Duran, P. and Pascual, C., Phase equilibria and ordering in the system HfO_2–Yb_2O_3. *J. Mater. Sci.*, 1984, **19**(4), 1178–1184.
163. Brown, F. N. and Duwez, P., Systems ZrO_2–La_2O_3 and ZrO_2–Nd_2O_3. *J. Am. Ceram. Soc.*, 1955, **38**(3), 95–101.
164. Roth, R. S., Pyrochlore-type compounds containing double oxides of trivalent and tetravalent ions. *J. Res. Nat. Bur. Stand.*, 1956, **56**(1), 17–25.
165. Perez-y-Jorba, M., ZrO_2-rare earth oxides systems. *Annu. Chim.*, 1962, **7**(7/8), 479–511.
166. Lin, T.-H. and Yu, H. C., Phase equilibria of the system La_2O_3–ZrO_2. *Kuei Suan Yen Hsueh Pao*, 1964, **3**(3), 159–166.
167. Michel, D., Perez-y-Jorba, M. and Colongues, R., Etude de la transformation ordre-desordre de la structure fluorite a la structure pyrochlore pour des phases $(1-x)$ ZrO_2–xLn_2O_3. *Mater. Res. Bull.*, 1974, **9**, 1457–1468.
168. Michel, D., Perez-y-Jorba, M. and Colongues, R., Growth from melting of zirconia rare earth oxide crystal. *J. Cryst. Growth*, 1978, **43**(34), 546–548.
169. Bastide, B., Odier, P. and Coutures, J. P., Phase equilibrium and martensitic transformation in lanthana-doped zirconia. *J. Am. Ceram. Soc.*, 1988, **71**(6), 449–453.
170. Rouanet, A., Etude des systemes zircone-oxyde de prazeodime et zircone-oxyde de terbium a haute temperature. *C. R. Acad. Sci. C.*, 1968, **286**, 1230–1233.
171. Strekalovski, V. N., Volchenkova, E. S. and Samarina, V. A., To investigation of the phase components in the system ZrO_2–$PrO_{1.83}$. *Izv. Akad. Nauk SSSR Neorg. Mater.*, 1965, **7**, 1372–1375.
172. Krasilnikov, M.D., Physicochemical investigation of the system zirconium dioxide–praseodymia–ytterbia, PhD, thesis, Institute Chemistry Silicates Akad. Nauk SSSR, Leningrad, 1978.
173. Glushkova, V. B., Davtyan, I. A. and Keler, E. K., Study of the system ZrO_2–Nd_2O_3. Study of the fields rich with neodymia. *Izv. Akad. Nauk SSSR Neorg. Mater.*, 1965, **1**, 1955–1964.
174. Davtyan, I. A., Glushkova, V. B. and Keler, E. K., Study of the system ZrO_2–Nd_2O_3. Study of the zirconia-rich fields. *Izv. Akad. Nauk SSSR Neorg. Mater.*, 1965, **1**, 743–750.
175. Sazonova, L. V., Davtyan, I. A. and Glushkova, V. B., Study of the system ZrO_2–Nd_2O_3 and effect of preparation on properties of the product. *Izv. Akad. Nauk SSSR Neorg. Mater.*, 1965, **1**, 1965–1977.
176. Dijk, T. V., de Vries, K. J. and Burggraf, A. J., Electrical conductivity of fluorite and pyrochlore $Ln_xZr_{1-x}O_{2-(x/2)}$ (Ln = Gd, Nd) solid solutions. *Phys. Status Solidi. A*, 1980, **58**, 115–125.
177. Volchenkova, Z. S., Phase relations in the system ZrO_2–Nd_2O_3. *Electrochemistry of Melted Salts and Solid Electrolytes*. UFAN SSSR, Sverdlovsk, 1970, pp. 125–128.
178. Michel, D., Rouaux, Y. and Perez-y-Jorba, M., Ceramic eutectics in the system ZrO_2–Ln_2O_3 (Ln—Lanthanide): unidirectional solidification, microstructural and crystallographic characterization. *J. Mater. Sci.*, 1980, **15**, 61–66.

179. Yoshimura, M., Yashima, M., Noma, T. and Somiya, S., Formation of diffusionlessly transformed tetragonal phases by rapid quenching of melts in ZrO_2–$RO_{1.5}$ systems (R = rare earths). *J. Mater. Sci.*, 1990, **25**(4), 2011–2016.
180. Stubican, V. S. and Hellmann, J. R., Phase equilibria in some zirconia systems. *Advances in Ceramics. Science and Technology of Zirconia*, In A. H. Heuer and L. W. Hobbs (ed.), The Am. Ceram. Soc., Columbus, OH, 1981, 3, pp. 25–36.
181. Kazuo, Sh., Masahiro, M., Koji, K. and Osamu, S., Oxigen-ion conduction in the $Sm_2Zr_2O_7$ pyrochlore phase. *J. Am. Ceram. Soc.*, 1979, **62**, 538–539.
182. Barry, E. S. and William, B., White characterization of anion disorder in zirconate $A_2B_2O_7$ compounds by Raman spectroscopy. *J. Am. Ceram. Soc.*, 1979, **62**, 468–469.
183. Glushkova, V. B. and Sazonova, L. V., Effect of rare-earth oxide dopants on polymorphism in zirconium dioxide. *Chemistry of High-Temperature Materials*. Nauka, Leningrad, 1967, pp. 83–90.
184. Davtyan, I. A., Glushkova, V. B. and Keler, E. K., Influence of europia dopants on polymorphism in zirconium dioxide. *Izv. Akad. Nauk SSSR Neorg. Mater.*, 1966, **2**(5), 890–897.
185. Portnoi, K. I., Timofeeva, N. I. and Salibekov, S. E., Synthesis and study of complex oxides and zirconia. *Izv. Akad. Nauk SSSR Neorg. Mater.*, 1972, **8**(2), 406–408.
186. Faucher, M. and Caro, P., Ordre et desordre dans certains composes du type pyrochlore. *J. Solid State Chem.*, 1975, **12**(1/2), 1–11.
187. Kiparisov, S. S., Belyaev, R. A., Belyakov, A. I., Bondarenko, V. V. *et al.*, The state diagram of the system Eu_2O_3–ZrO_2. *Izv. Akad. Nauk SSSR Neorg. Mater.*, 1976, **12**(9), 1693–1694.
188. Moore, D. A. and Fergusson, F., Zirconia stabilized cubic europia. *J. Am. Ceram. Soc.*, 1982, **65**(9), 414–418.
189. Scott, H. G., On the continuous transition between two structure types in the zirconia–ghadolinia system. *J. Mater. Sci.*, 1978, **13**, 1592–1593.
190. Mogira, T., Emura, S., Yoshiasa, A., Kikkawa, S., Kanamaru, F. and Koto, K., X-ray and Raman study of coordination states of fluorite- and pyrochlore-type compounds in the system ZrO_2–Gd_2O_3. *Solid State Ionics*, 1990, **40**, 357–361.
191. Leung, D. K., Chan, C. J., Ruhle, M. and Lange, F. F., Metastable crystallization phase partitioning and grain growth of ZrO_2–Gd_2O_3 materials processed from liquid precursors. *J. Am. Ceram. Soc.*, 1991, **74**(11), 2786–2792.
192. Karaulov, A. G., Zoz, E. I. and Shlyahova, T. M., New refractory material from zirconium dioxide, stabilized with gadolinium oxide. In *Proceedings of the All-Union. Conference Zirconium Oxide*, 1991, p. 54.
193. Ceder, G., Tepesch, P. D., Kohan, A. F. and Van der Ven, A., A model to predict ionic disorder and phase diagrams: application to Ca–MgO, Gd_2O_3–ZrO_2, and sodium-*b*-alumina. *J. Electroceram.*, 1997, **1**, 15–26.
194. Pascual, C. and Duran, P., Phase relations and ordering in the dysprosia–zirconia system. *J. Mater. Sci.*, 1980, **15**, 1701–1708.
195. Andrievskaya, E. R., Red'ko, V. P., Smirnov, V. P. and Lopato, L. M., Advanced ceramic based on the ternary systems $ZrO_2(HfO_2)$–Y_2O_3–Eu_2O_3. *Key Engeneering Materials, Part II*, 206–213, 2002, Trans Tech Publications Ltd., Brandrain 6, CH-8707 Veticon-Zurich, Switzerland, pp. 1113–1116.
196. Lopato, L. M., Andrievskaya, E. R., Shevchenko, A. V. and Red'ko, V. P., Phase relations in the system ZrO_2–Eu_2O_3. *Zh. Neorg. Khim.*, 1997, **42**(10), 1736–1739.
197. Duwez, P. S., Brown, F. N. and Odell, F., The zirconia–yttria system. *J. Electrochem. Soc.*, 1951, **98**(9), 356–358.
198. Fan, F.-K., Kuznetsov, A. K. and Keler, E. K., Phase relations in the system Y_2O_3–ZrO_2. *Izv. Akad. Nauk SSSR Ser. Chem.*, 1962, **7**, 1141–1146.
199. Fan Fu-Kan, Kuznetsov, A. K. and Keler, E. K., Phase relations in the system Y_2O_3–ZrO_2. *Izv. Akad. Nauk SSSR Ser. Chem.*, 1963, **4**, 601–610.
200. Lin, T.-H. and Yu, H. C., Phase equilibria of the system Y_2O_3–ZrO_2. *Kuei Suan Gen Hsueh PaO*, 1965, **4**(1), 22–29.
201. Noguchi, T., Mizuno, M. and Yamada, T., Liquidus curve of the zirconium–yttrium oxide system as measured by solar furnace. *Bull. Chem. Soc. Jpn.*, 1970, **43**, 2614–2616.
202. Smith, D. K. and Newkirk, H. W., The crystal structure of baddeleyte and its reaction to the polymorphism of ZrO_2. *Acta Cryst.*, 1965, **18**, 983–991.
203. Smith, D. K., The nonexistence of yttrium zirconate. *J. Am. Ceram. Soc.*, 1966, **49**(11), 625–627.
204. Steele, D. and Fender, B., The structure of cubic ZrO_2–$YO_{1.5}$ solid solutions by neutron scattering. *J. Phys. C: Solid State Phys.*, 1974, **7**(1), 1–11.
205. Srivastava, K. K., Patil, R. N., Chroundary, C. B. *et al.*, Revised phase diagram of the system zirconium oxide (ZrO_2–$YO_{1.5}$). *J. Br. Ceram. Soc.*, 1974, **73**(3), 85–91.
206. Scott, H. G., Phase relationships in the zirconia–yttria system. *J. Mater. Sci.*, 1975, **10**(7), 1527–1535.
207. Scott, H. G., Phase relationships in the yttria-rich part of the yttria–zirconia system. *J. Mater. Sci.*, 1977, **12**(2), 311–316.
208. Stubican, V. S., Hink, R. C. and Ray, S. P., Phase equilibria and ordering in the system ZrO_2–Y_2O_3. *J. Am. Ceram. Soc.*, 1978, **61**(1/2), 17–21.
209. Pascual, C. and Duran, P., Subsolidus phase equilibria and ordering in the system ZrO_2–Y_2O_3. *J. Am. Ceram. Soc.*, 1983, **66**(1), 23–27.
210. Scott, H. G., The yttria–zirconia δ-phase. *Acta Cryst. B*, 1977, **33**(1), 281–282.
211. Rouanet, A., High-temperature solidification and phase diagrams of the ZrO_2–Er_2O_3, ZrO_2–Y_2O_3 and ZrO_2–Yb_2O_3 systems. *C. R. Acad. Sci. Ser. C*, 1968, **267**(23), 1581–1584.
212. Ray, S. P. and Stubican, V. S., Fluorite related ordered compounds in the ZrO_2–Y_2O_3 system. *Mater. Res. Bull.*, 1977, **12**(5), 549–554.
213. Ruh, R., Mazdiyashi, K. S., Valentine, P. G. and Bielstein, H. O., Phase relations in the system ZrO_2–Y_2O_3 at low Y_2O_3 contents. *J. Am. Ceram. Soc.*, 1984, **69**(9), 190–192.
214. Katamura, J. and Sakuma, T., Thermadynamic analysis of the cubic-tetragonal phase equilibria in the system ZrO_2–$YO_{1.5}$. *J. Am. Ceram. Soc.*, 1997, **80**(10), 2685–2688.
215. Katamura, J., Seki, T. and Sakuma, T., The cubic–tetragonal phase equilibria in the ZrO_2–R_2O_3 (R = Nd, Sm, Gd, Y). *J. Phase Equilibr.*, 1995, **16**(4), 315–319.
216. Lanteri, V., Heuer, A. H. and Mitchell, T. E., Tetragonal phase in the system ZrO_2–Y_2O_3 in advanced ceramics. *Science and Technology of Zirconia II*, In N. Claussen, M. Ruhle, A. H. Heuer (ed.), Am. Ceram. Soc., OH, 1984, 12, pp. 118–130.
217. Gonzalez, M., Moure, C., Jurado, J. R. and Duran, P., Solid state reaction, microstructure and phase relations in the ZrO_2-rich region of the ZrO_2–Yb_2O_3 system. *J. Mater. Sci.*, 1993, **28**, 3451–3456.
218. Duran, P., The system erbia–zirconia. *J. Am. Ceram. Soc.*, 1977, **60**(11–12), 510–513.
219. Pascual, C. and Duran, P., Phase equilibria and ordering in the erbia–zirconia system. *J. Mater. Sci.*, 1981, **16**(11), 3067–3076.
220. Yashima, M., Noma, T., Ishizava, N. and Yoshimura, M., Stable and metastable phase relationships in the system ZrO_2–$ErO_{1.5}$. *J. Am. Ceram. Soc.*, 1991, **74**(3), 510–513.
221. Andrievskaya, E. R., Lopato, L. M. and Shevchenko, A. V., Phase relations in the ZrO_2–Y_2O_3–Er_2O_3 system. *Izv. RAN Neorg. Mater.*, 1996, **32**(6), 721–726.
222. Glushkova, V. B., *Polymorphism of the Rare-Earth Oxides*. Nauka, Leningrad, 1967, p. 134.
223. Foex, M. and Traverse, J. P., Remarques sur les transformation cristallines presenties a hautes temper. *Refract. Rev. Intern. Hautes Temper. Refract.*, 1966, **3**(4), 429–453.
224. Aldebert, P. and Traverse, J. P., Etude pardiffraction neutronique des structures de haute temperature de La_2O_3 et Nd_2O_3. *J. Mater. Res. Bull.*, 1979, **14**(5), 303–323.
225. Lopato, L. M., Shevchenko, A. V., Kuschevski, A. E. and Tresvyatski, S. G., Polymorphous transformations in the REO at high temperature. *Izv. Akad. Nauk SSSR Neorg. Mater.*, 1974, **10**(8), 1481–1484.
226. Traverse, J. P., Etude du Polymorphisme des Sesquioxides de Terres Rares: These, Grenoble, 1971, p. 150.
227. Tabira, Y., Withers, R. L., Barry, J. C. and Elcoro, L., The strain-driven pyrochlore to "defect fluorite" phase transition in rare earth sesquioxide stabilized cubic zirconias. *J. Solid State Chem.*, 2001, **159**, 121–129.
228. Yashima, M., Ohtake, K., Kakihana, M., Arashi, H. and Yoshimura, M., Determination of tetragonal–cubic phase boundary of $Zr_{1-x}R_xO_{2-(x/2)}$

(R = Nd, Sm, Y, Er, and Yb) by Raman scattering. *J. Phys. Chem. Solids*, 1996, **57**, 17–24.
229. Yashima, M., Noma, T., Ishizava, N. and Yoshimura, M., Effects of non-compositional inhomogeneity on t–m phase transformation during grinding of various rare-earth-doped zirconias. *J. Am. Ceram. Soc.*, 1991, **74**, 3011–3016.
230. Yashima, M., Hirose, T., Kakihona, M., Suzuki, Y. and Yoshimura, M., Size and charge effects of dopant M on the unit cell parameters of monoclinic zirconia solid solutions $Zr_{0.98}M_{0.02}O_{2-\delta}$ (M = Ce, La, Nd, Sm, Y, Er, Yb, Sc, Mg, Ca). *J. Am. Ceram. Soc.*, 1997, **80**(1), 171–175.
231. Kim, D.-J., Lattice parameters, ionic conductivities and solubility limits in fluorite-structure MO_2 oxide ($M = Hf^{4+}$, Zr^{4+}, Ce^{4+}, Th^{4+}, U^{4+}) solid solutions. *J. Am. Ceram. Soc.*, 1989, **72**(8), 1415–1421.
232. Glushkova, V. B., *Study of Kinetics for Kinetics of Solid State Transformations in the Systems with Refractory Oxides*. Progress in Physics and Chemistry of Silicates, Nauka, Leningrad, 1978, pp. 133–161.
233. Scherbakova, L. G., Glushkova, V. B. and Sapozhnikov, R. A., Synthesis of solid solutions based on HfO_2 and ZrO_2 and study of their crystallization. *Izv. Akad. Nauk SSSR Neorg. Mater.*, 1977, **13**, 674–677.
234. Glushkova, V. B., Grischenko, V. I., Krzhizhanovskaya, V. A. and Keler, E. K., Study of the kinetics on the initial stage of solid solution formation in the systems Ln_2O_3–HfO_2 (Ln = Nd, Sm, Dy). *Izv. Akad. Nauk SSSR Neorg. Mater.*, 1976, **12**, 695–697.
235. Collong, R., *Non-Stoichiometry*. Mir, Moskow, 1974, p. 288 [in Russian].
236. Tabira, Y. and Withers, R. L., Structure and crystal chemistry as a function of composition across the wide range nonstoichiometric $(1-\varepsilon)ZrO_2$–$\varepsilon SmO_{1.5}$ $0.38 < \varepsilon < 0.55$, oxide pyrochlore system. *J. Solid State Chem.*, 1999, **148**, 205–214.
237. Subramanian, M. A., Aravamudan, G. and Subba Rao, G. V., Oxide pyrochlores—a review. *Prog. Solid State Chem.*, 1983, **15**, 55–143.
238. Norby, T., Fast oxygen ion conductors—from doped to ordered system. *J. Mater. Chem.*, 2001, **11**, 11–18.
239. Minervini, L., Grimes, R. W. and Sickafus, K. E., Disorder in pyrochlore oxides. *J. Am. Ceram. Soc.*, 2000, **83**(8), 1873–1878.
240. Lian, J., Wang, L. M., Wang, S. X., Chen, J., Boatner, L. A. and Ewing, R. C., Nanoscale manipulation of pyrochlore: new nanocomposite ionic conductors. *Phys. Rev. Lett.*, 2001, **87**(14), 1–4, 145901.
241. Wilde, P. J. and Catlow, C. R. A., Defect and diffusion in pyrochlore structured oxides. *Solid State Ionics*, 1998, **112**, 173–183.
242. Wilde, P. J. and Catlow, C. R. A., Molecular dynamics, study of the effect of doping and disorder on diffusion in gadolinium zirconate. *Solid State Ionics*, 1998, **112**, 185–195.
243. Berndt, U., Maier, D. and Keller, C., Phasengleichgenwichte in interlanthanidenoxid systemen. *J. Solid State Chem.*, 1976, **16**(1–2), 189–195.
244. Lopato, L. M., Nigmanov, B. S., Shevchenko, A. V. and Zaitseva, Z. A., Reaction of lanthanum oxide with yttrium oxide. *Izv. Akad. Nauk SSSR Neorg. Mater.*, 1986, **22**(5), 771–774.
245. Shevchenko, A. V., Nigmanov, B. S., Zaitseva, Z. A. and Lopato, L. M., Interaction of samaria and gadolinia with yttria. *Izv. Akad. Nauk SSSR Neorg. Mater.*, 1986, **22**(5), 775–778.
246. Nigmanov, B. S., Shevchenko, A. V., Zaitseva, Z. A. and Lopato, L. M., Reaction of dysprosium oxide with yttrium oxide. *Izv. Akad. Nauk SSSR Neorg. Mater.*, 1986, **22**(5), 780–785.
247. Maister, I. M., Lopato, L. M., Shevchenko, A. V. and Nigmanov, B. S., The system Y_2O_3–Er_2O_3. *Izv. Akad. Nauk SSSR Neorg. Mater.*, 1984, **20**(3), 446–448.
248. Andrievskaya, E. R., Zaitseva, Z. A., Shevchenko, A. V. and Lopato, L. M., Phase diagram of the Eu_2O_3–Y_2O_3 system. *Izv. Akad. Nauk SSSR Neorg. Mater.*, 1997, **33**(4), 465–468.
249. Berndt, V., Maier, D. and Keller, C., New $A'''B'''O_3$ interlanthanide perovskite compounds. *J. Solid State Chem.*, 1975, **13**(1–2), 131–135.
250. Mizuno, M., Rouanet, A., Yamada, T. and Noguchi, T., Phase diagram of the system La_2O_3–Y_2O_3 at high temperatures. *J. Ceram. Soc. Jpn.*, 1976, **84**(7), 342–347.
251. Coutures, J. and Foex, M., Etude a haute temperature du diagrama d' equilibrie du systeme forme par le sesquioxyde d'yttrium. *J. Solid State Chem.*, 1974, **11**(4), 294–300.
252. Wei, G. C., Emma, T. and Rhodes, W. H., Analytical microscopy study of phases and fracture in Y_2O_3–La_2O_3 alloys. *J. Am. Ceram. Soc.*, 1988, **71**(10), 820–825.
253. Rhodes, W. H., Controlled transient solid second phase sintering of yttria. *J. Am. Ceram. Soc.*, 1981, **64**(1), 13–17.
254. Tikhonov, P. A., Merezhinski, K. Yu. and Kuznetsov, A. K., Solid solution in the system Y_2O_3–Pr_2O_3 and their morphotropism. *Dokl. Akad. Nauk SSSR Phys. Chem.*, 1975, **222**(6), 1387–1389.
255. Coutures, J., Verges, R. and Foex, M., Etude a haute temperature des systemes formes par le sesquioxyde de neodyme avec les sesquioxides d' yttrium et d' ytterbium. *Mater. Res. Bull.*, 1974, **9**(12), 1603–1612.
256. Hayek, B., Kalalova, E. and Stompfova, H. O., Tvorbe Smesnych krystalu v systemech Sm_2O_3–Y_2O_3, Sm_2O_3–Tb_2O_3 a Sm_2O_3–Dy_2O_3. *Prispevky k chemii vcachejsich prvku, Vys. skoly Chem.-Technol., Praha, B*, 1972, **14**, p21.
257. Ahrens, L. H., Use of ionization potentials I ionic radii of the elements. *Geochim. Cosmochim. Acta*, 1952, **2**, 155–158.